Computer Aided Analysis of Filters Using Level Set Segmentation for Biomedical Images

Thesis submitted in

partial fulfillment of the requirement for the award of degree of

Master of Engineering
in
Electronics Instrumentation and Control

Submitted by:

Shweta Gupta

(80751023)

Under Esteemed Guidance of:

Dr. Yaduvir Singh

Associate Professor, EIED

Thapar University, Patiala.

JUNE 2009

ELECTRICAL AND INSTRUMENTATION ENGINNERING DEPARTMENT
THAPAR UNIVERSITY
PATIALA – 147004

DECLARATION

*I hereby declare that the report entitled "**Computer Aided Analysis of Filters using Level Set Segmentation for Biomedical Images**" is an authentic record of my own work carried out as requirements for the award of degree of **Master of Engineering** in **Electronic Instrumentation & Control** at **Thapar University**, Patiala, under the guidance of **Dr. Yaduvir Singh** (Associate Professor, EIED during January to June 2009.*

Shweta Gupta

Shweta Gupta

Date: 15/07/09

Roll. No. 80751023

It is certified that the above statement made by the student is correct to the best of my knowledge and belief.

Dr. Yaduvir Singh
Associate Professor, EIED
(Supervisor)
Thapar University, Patiala

S. Ghosh

Dr. Smarajit Ghosh
Professor & Head, EIED
Thapar University, Patiala.

RKSharma 21/7/09

Dr. R. K. Sharma
Dean of Academic Affairs
Thapar University, Patiala.

ACKNOWLEDGMENT

The real spirit of achieving a goal is through the way of excellence and austere discipline. I would have never succeeded in completing my task without the cooperation, encouragement and help provided to me by various personalities.

With deep sense of gratitude I express my sincere thanks to my esteemed and worthy supervisors, Dr. Yaduvir Singh, Associate Professor, Department of Electrical & Instrumentation Engineering, Thapar University, Patiala, for their valuable guidance in carrying out this work under their effective supervision, encouragement, enlightenment and cooperation.

I shall be failing in my duties if I do not express my deep sense of gratitude towards Mr. Smarajit Ghosh, Professor & Head of the Department of Electrical & Instrumentation Engineering, Thapar University, Patiala who has been a constant source of inspiration for me throughout this work.

I am also grateful to Dr. R. K. Sharma, Dean of Academic Affair for his constant encouragement that was of great importance in the completion of the thesis.

I extend my thanks to Dr. Abhijit Mukherjee, Director, Thapar University for his valuable support that made me consistent performer.

I am also thankful to all the staff members of the Department for their full cooperation and help.

This acknowledgement would be incomplete if I do not mention the emotional support and blessing provided by my friends for their kind co-operation.

My greatest thanks are to all who wished me success especially my parents. Above all I render my gratitude to the ALMIGHTY who bestowed self-confidence, ability and strength in me to complete this work.

Shweta Gupta

Place: Thapar University, Patiala *Shweta Gupta*

Date: 15/07/09

ABSTRACT

Medical imaging allows scientist and physicians to decide about life saving information regard to the human physiological activities. It plays an important role in the diagnosis, therapy and treatment of various organs, tumors and other abnormalities. Image segmentation is typically used to locate objects and boundaries in images and should stop when the object of interest in an application have been isolated .It is used to calculate the geometric shape and size of tumors and abnormal growth of any tissue. There are many techniques available for auto-segmentation of images like Active contours, Fuzzy based classifiers, Gradient Vector Field theory, Tensor based segmentation, Level set theory etc. But many of them are suffering from problems like optimization, initialization and insufficient results in noisy images. Most widely used segmentation is level set segmentation in biomedical medical images such as X-ray, CT and MRI.

In this work we have applied various image filtering techniques to modify or to smooth the image and to enhance the efficiency of previous algorithm. Therefore, the use of filter depends upon the type of images used for the calculation of tumor size and shape, in the X- ray, CT scan and MRI images. For the evaluation of the performance of filters the following parameters like signal to noise ratio, peak signal to noise ratio, weighted peak signal to noise ratio, entropy and energy measure are used and the MATLAB codes required in calculating these parameters are developed. These parameters are used to calculate the image quality of the output image obtained from above mentioned filters. However, only a few filters gave good results. We tried to calculate the parameters of the segmented part and optimum filter for above said purpose.

ORGANIZATION OF THESIS

Chapter1-This chapter introduces basic concepts the digital images and also the brief review of the digital image processing .It focuses on the various methods of image segmentation.

Chapter2-The second chapter is the review of the literature.

Chapter3-This chapter is based on medical imaging, in which various medical imaging techniques are briefed and CT scan, X-ray and MRI imaging process is discussed in detail.

Chapter4-This chapter formulates the problem and discusses the proposed solution with detailed study of level set segmentation and spatial filtering techniques.

Chapter5-This chapter is based on the methodology used in this work. It gives the modified algorithm which is used to complete this work.

Chapter6-This chapter is the simulation and testing of the various images.

Chapter7- Conclusion of the thesis with future scope.

TABLE OF CONTENTS

Contents **Page No**

LIST OF FIGURES

LIST OF TABLES

LIST OF ABBREVIATIONS

PCNN	Pulse-Coupled Neural Networks
2-D	2-Dimensional
EM	Expectation maximization
PDE	Partial differential equation
ADI	Alternating direction implicit
CTA	Computed tomography angiography
MRI	Magnetic resonance imaging
CT	Computed tomography
SRG	Seeded region growing
CTA	Computed tomography angiography
HARP	Harmonic Phase reference
LSM	Level set method
NMR	Nuclear magnetic resonance
RF	Radio-frequency
PET	Positron emission tomography
IVU	Intravenous urogram
OPG	Orthopantomography
CAT	Computed Axial Tomography
SNR	Signal to noise ratio
PSNR	Peak signal to noise ratio
WPSNR	Weighted peak signal to noise ratio

CHAPTER 1

INTRODUCTION

A digital image is a representation of a two-dimensional image as a finite set of digital values. In image processing, the digitization process includes sampling and quantization of continuous data. The sampling process samples the intensity of the continuous-tone image, such as a monochrome, color or multi-spectrum image, at specific locations on a discrete grid. The grid defines the sampling resolution. The quantization process converts the continuous or analog values of intensity brightness into discrete data, which corresponds to the digital brightness value of each sample, ranging from black, through the grays, to white. A digitized sample is referred to as a picture element, or pixel. The digital image contains a fixed number of rows and columns of pixels. Pixels are like little tiles holding quantized values that represent the brightness at the points of the image. Pixels are parameterized by position, intensity and time. Typically, the pixels are stored in computer memory as a raster image or raster map, a two-dimensional array of small integers. Image is stored in numerical form which can be manipulated by a computer. A numerical image is divided into a matrix of pixels (picture elements).

Figure 1.1: Digitization of a continuous image

1.1 Brief review of Digital Image Processing

We are in the midst of a visually enchanting world, which manifests itself with a variety of forms and shapes, colors and textures, motion and tranquility. The human perception has the capability to acquire, integrate, and interpret all this abundant visual information around us. It is challenging to impart such capabilities to a machine in order to interpret the visual information embedded in still images, graphics, and video or moving images in our sensory world. It is thus important to understand the techniques of storage, processing, transmission, recognition, and finally interpretation of such visual scenes. A two-dimensional image that is recorded by sensors is the mapping of the three-dimensional visual world.

1.2 Image processing operations

Image processing operations can be roughly divided into three major categories:

a) Image Restoration

b) Image Enhancement

c) Image Compression

d) Image Segmentation

1.2.1 Image Restoration:

It takes a corrupted image and attempts to recreate a clean image. As many sensors are subject to noise, they results in corrupted images that don’t reflect the real world scene accurately and old photograph and film archives often show considerable damage.

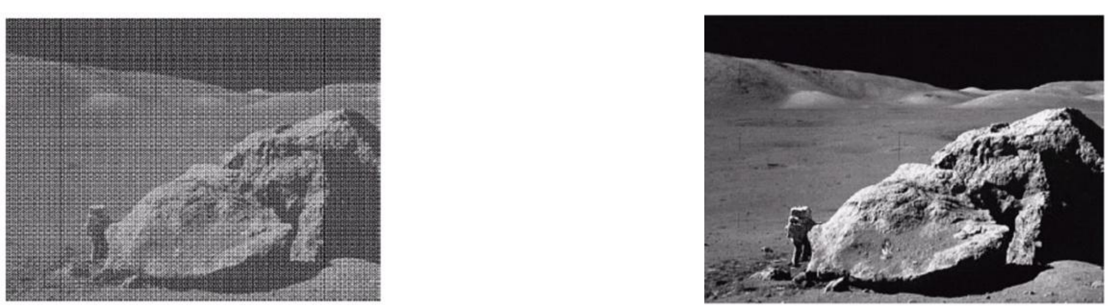

(a) (b)

Figure 1.2: (a) Image before restoration (b) image after restoration

1.2.2 Image Enhancement:

It alters an image to makes it's meaning clearer to human observers. It is often used to increase the contrast in images that are substantially dark or light. Enhancement algorithms often play attention to human sensitivity to contrast.

(a)

(b)

Figure 1.3: (a) Image before enhancement (b) image after enhancement

1.2.3 Image Compression:

It is the process that helps to represent image data with as few bits as possible by exploiting redundancies in the data while maintaining an appropriate level of quality for the user. The human eye has less spatial sensitivity to color than for luminance information. Large amounts of data are used to represent an image, so image has to be compressed when transferring from one place to another. Transform Coding has been a very popular technique for digital image compression. It is used in the International Standard for Still Image Compression -JPEG (Joint Photographic Experts Group).

(a)

(b)

Figure 1.4: (a) 1mage before compression (b) Image after compression

1.2.4 Image Segmentation:

It is the process that subdivides an image into a number of uniformly homogeneous regions. Each homogeneous region is a constituent part or object in the entire scene. The principal areas of interest within this category are the detection of edges of a digital image.

(a) (b)

Figure 1.5: (a) Image before segmentation (b) Image after segmentation

1.3 Segmentation

Segmentation refers to the process of partitioning a digital image into multiple segments. It subdivides an image into it's constitute regions or object. The goal of segmentation is to simplify and change the representation of an image into something that is more meaningful and easier to analyze. Segmentation should stop when the object of interest in an application have been isolated. Image segmentation is typically used to locate objects and boundaries (lines, curves, etc.) in images. More precisely, image segmentation is the process of assigning a label to every pixel in an image such that pixels with the same label share certain visual characteristics. Segmentation of nontrivial images is one of the most difficult tasks in image processing.

The result of image segmentation is a set of segments that collectively cover the entire image, or a set of contours extracted from the image. Each of the pixels in a region is similar with respect to some characteristic or computed property, such as color, intensity or texture. Adjacent regions are significantly different with respect to the same characteristics.

Some of the practical applications of medical image segmentation are:

- Locate tumors and other pathologies
- Measure tissue volumes
- Computer-guided surgery
- Diagnosis
- Treatment planning
- Study of anatomical structure

Some other applications are:

- Locate objects in satellite images (roads, forests, etc.)
- Face recognition
- Fingerprint recognition
- Traffic control systems
- Brake light detection
- Machine vision

1.4 Methods of image segmentation

Several general-purpose algorithms and techniques have been developed for image segmentation. These techniques often have to be combined with domain knowledge in order to effectively solve an image segmentation problem for problem domain. These are listed below:

1.4.1 Clustering methods

The K-means algorithm is an iterative technique that is used to partition an image into K clusters. The basic algorithm is:

1. Choose the number of clusters, K.
2. Pick K cluster centers, either randomly or based on some heuristic
3. Assign each pixel in the image to the cluster that minimizes the variance between the pixel and the cluster center
4. Re-compute the cluster centers by averaging all of the pixels in the cluster
5. Repeat steps 2 and 3 until convergence is attained (e.g. no pixels change clusters)

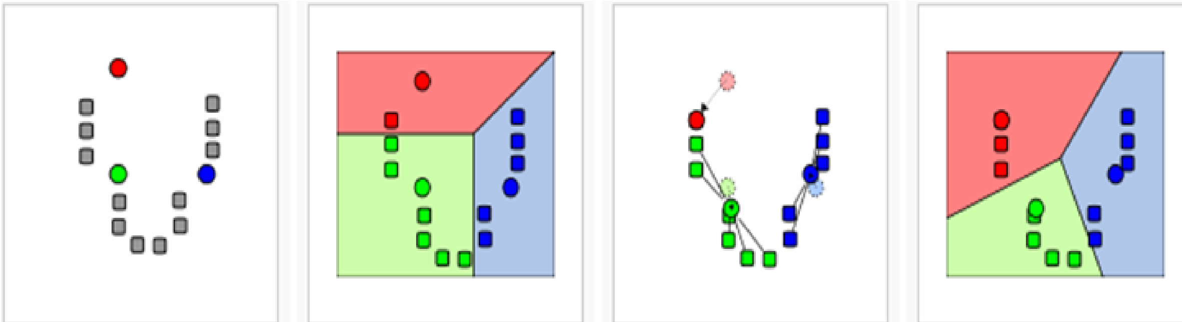

Show the initial randomized centroids and no. of points

points are associated with the nearest centroid

now the centroids are moved to the centre of their respective clusters.

step 2 and 3 are repeated until a suitable level of convergence has been reached

Figure 1.6: K-means clustering

The quality of the final solution of this algorithm depends largely on the initial set of clusters, and may, in practice, be much poorer than the global optimum. Since the algorithm is extremely fast, a common method is to run the algorithm several times and return the best clustering found. A drawback of the k-means algorithm is that the number of clusters k is an input parameter. An inappropriate choice of k may yield poor results. The algorithm also assumes that the variance is an appropriate measure of cluster scatter.

1.4.2 Histogram Based Method

Histogram-based methods are very efficient when compared to other image segmentation methods because they typically require only one pass through the pixels. In this technique, a histogram is computed from all of the pixels in the image, and the peaks and valleys in the histogram are used to locate the clusters in the image. Color or intensity can be used as the measure. A refinement of this technique is to recursively apply the histogram-seeking method to clusters in the image in order to divide them into smaller clusters. This is repeated with smaller and smaller clusters until no more clusters are formed.

One disadvantage of the histogram-seeking method is that it may be difficult to identify significant peaks and valleys in the image. In this technique of image classification distance metric and integrated region matching are familiar.

1.4.3 Edge detection method

Edge detection techniques have therefore been used as the base of another segmentation technique. It is a well-developed field on its own within image processing. Region boundaries and edges are closely related, since there is often a sharp adjustment in intensity at the region boundaries. The result of applying an edge detector to an image may lead to a set of connected curves that indicate the boundaries of objects, the boundaries of surface markings as well curves that correspond to discontinuities in surface orientation. Thus, applying an edge detector to an image may significantly reduce the amount of data to be processed and may therefore filter out information that may be regarded as less relevant, while preserving the important structural properties of an image. The edges identified by edge detection are often disconnected. To segment an object from an image however, one needs closed region boundaries. Discontinuities are bridged if the distance between the two edges is within some predetermined threshold

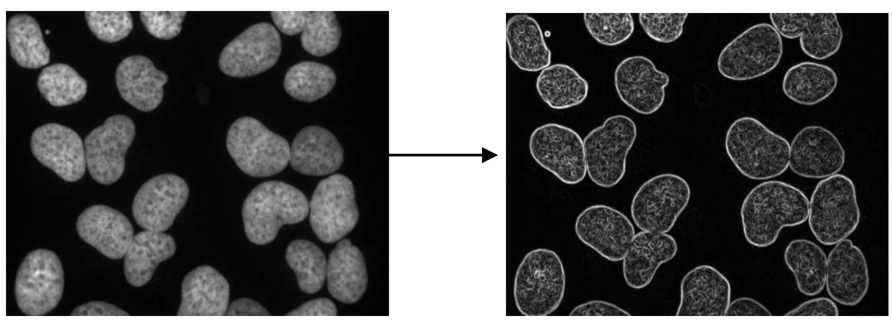

Figure 1.7: Example of edge detection method

The edges extracted from a two-dimensional image of a three-dimensional scene can be classified as:

Viewpoint dependent: Viewpoint dependent edge may change as the viewpoint changes, and typically reflects the geometry of the scene, such as objects occluding one another

Viewpoint independent: A viewpoint independent edge typically reflects inherent properties of the three-dimensional objects, such as surface markings and surface shape.

1.4.4 Region growing method

The first region growing method was the seeded region growing method. This method takes a set of seeds as input along with the image. The seeds mark each of the objects to be segmented. The regions are iteratively grown by comparing all unallocated neighbouring pixels to the regions. The difference between a pixel's intensity value and the region's mean, δ, is used as a measure of similarity. The pixel with the smallest difference measured this way is allocated to the respective region. This process continues until all pixels are allocated to a region.

Seeded region growing requires seeds as additional input. The segmentation results are dependent on the choice of seeds. Noise in the image can cause the seeds to be poorly placed. Unseeded region growing is a modified algorithm that doesn't require explicit seeds. It starts off with a single region A_1 – the pixel chosen here does not significantly influence final segmentation. At each iteration , it considers the neighboring pixels in the same way as seeded region growing. It differs from seeded region growing in that if the minimum δ is less than a predefined threshold T then it is added to the respective region A_j. If not, then the pixel is considered significantly different from all current regions A_i and a new region A_{n+1} is created with this pixel.

One variant of this technique is based on pixel intensities. The mean and scatter of the region and the intensity of the candidate pixel is used to compute a test statistic. If the test statistic is sufficiently small, the pixel is added to the region, and the region's mean and scatter are recomputed. Otherwise, the pixel is rejected, and is used to form a new region.

1.4.5 Level set method

The level set method was initially proposed to track moving interfaces in 1988 and has spread across various imaging domains in the late nineties. It can be used to efficiently address the problem of curve/surface/etc. propagation in an implicit manner. The central idea is represent the evolving contour using a signed function, where its zero level corresponds to the actual contour. Then, according to the motion equation of the contour, one can easily derive a similar flow for the implicit surface that when applied to the zero-level will reflect the propagation of the contour. The level set method evolves a contour (in two dimensions) or a surface (in three dimensions) implicitly by manipulating a higher dimensional function, called the level set function Φ(x, t). The evolving contour or surface can be extracted from the zero level set .The level set method encodes numerous advantages: it is implicit, parameter free, provides a direct way to estimate the geometric properties of the evolving structure, can change the topology and is intrinsic. Therefore, one can conclude that it is a very convenient framework to address numerous applications of computer vision and medical image analysis

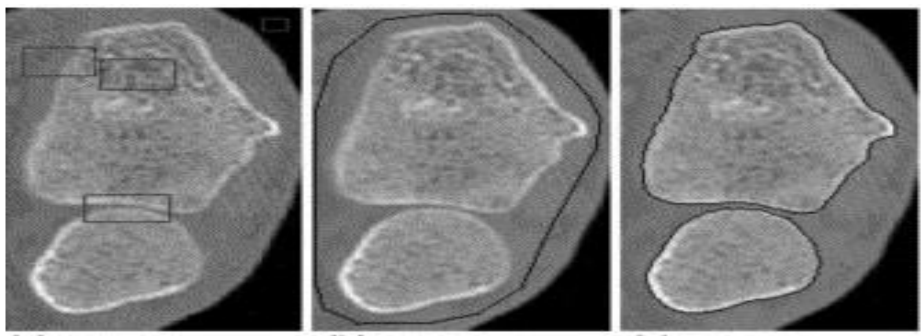

Figure 1.8: Segmentation of bone from CT image by level set segmentation: (a) carpal bone; (b) initial curve; (c) the result of level segmentation

In the level set method, the curve is represented implicitly as a level set of a 2D scalar function referred to as the level set function which is usually defined on the same domain as the image. The level set is defined as the set of points that have the same function value. It is worth noting that the level set function is different from the level sets of images, which are sometimes used for image enhancement. The sole purpose of the level set function is to provide an implicit representation of the evolving curve.

1.4.6 Graph partitioning methods

Graphs can effectively be used f0r image segmentation. Usually a pixel or a group of pixels are vertices and edges define the similarity or dissimilarity among the neighborhood pixels. Some popular algorithms of this category are random walker, minimum mean cut, minimum spanning tree-based algorithm, normalized cut, etc. The normalized cuts method, the image being segmented is modeled as a weighted, undirected graph .Each pixel is a node in the graph, and an edge is formed between every pair of pixels. The weight of an edge is a measure of the similarity between the pixels. The image is partitioned into disjoint sets (segments) by removing the edges connecting the segments. The optimal partitioning of the graph is the one that minimizes the weights of the edges that were removed the cut. This algorithm seeks to minimize the normalized cut, which is the ratio of the cut to all of the edges in the set.

1.4.7 Multi- scale segmentation

Multi- scale segmentation a general framework for signal and image segmentation, based on the computation of image descriptors at multiple scales of smoothing. Segmentation criteria can be arbitrarily complex and may take into account global as well as local criteria. A common requirement is that each region must be connected in some sense.

The notion that a one-dimensional signal could be unambiguously segmented into regions, with one scale parameter controlling the scale of segmentation. A key observation is that the zero-crossings of the second derivatives (minima and maxima of the first derivative or slope) of multi-scale-smooth versions of a signal form a nesting tree, which defines hierarchical relations between segments at different scales. Specifically, slope extreme at coarse scales can be traced back to corresponding features at fine scales. When a slope maximum and slope minimum annihilate each other at a larger scale, the three segments that they separated merge into one segment, thus defining the hierarchy of segments.

1.4.8 Semi-automatic segmentation

In this kind of segmentation, the user outlines the region of interest with the mouse clicks and algorithms are applied so that the path that best fits the edge of the image is shown. Techniques like Livewire or Intelligent Scissors are used in this kind of segmentation.

Livewire: Livewire is a segmentation technique which allows regions of interest to be extracted quickly and accurately, using simple mouse clicks. It is based on the lowest cost path algorithm. Firstly the grayscale image is modeled as a rectangular matrix whose pixel values are integers ranging from 0 to 255 (if the image is a color one, it might be converted to a grayscale one and use the algorithm the same way, although it's better to maximize the costs on each color channel). Each pixel of the matrix is a vertex of the graph and has edges going to the 8 pixels around it, as up, down, left, right, upper-right, upper-left, down-right, down-left. The edge costs are defined based on a cost function.

The user sets the starting point clicking on an image's pixel. Then, starts to move the mouse over other points, the smallest cost path is drawn from the starting pint to the pixel where the mouse is over, changing itself if the user moves the mouse. To choose the path that is being displayed, simply clicks the image again.One can easily see in the right image, that the places where the user clicked to outline the desired region of interest are marked with a small square. It is also easy to see that the livewire has snapped on the image's borders.

Figure 1.9: livewire segmentation on a baby's photo

1.4.9 Neural network segmentation

Neural Network segmentation relies on processing small areas of an image using an artificial neural network or a set of neural networks. After such processing the decision-making mechanism marks the areas of an image accordingly to the category recognized by the neural network

Pulse-Coupled Neural Networks (PCNNs) are neural models and developed for high-performance biometic image processing. PCNNs have been utilized for a variety of image processing applications, including: image segmentation, feature generation, face extraction, motion detection, region growing, noise reduction, and so on. A PCNN is a two-dimensional neural network. Each neuron in the network corresponds to one pixel in an input image, receiving its corresponding pixel's color information (e.g. intensity) as an external stimulus. Each neuron also connects with its neighboring neurons, receiving local stimuli from them. The external and local stimuli are combined in an internal activation system, which accumulates the stimuli until it exceeds a dynamic threshold, resulting in a pulse output. Through iterative computation, PCNN neurons produce temporal series of pulse outputs. The temporal series of pulse outputs contain information of input images and can be utilized for various image processing applications, such as image segmentation and feature generation. Compared with conventional image processing means, PCNNs have several significant merits, including robustness against noise, independence of geometric variations in input patterns, capability of bridging minor intensity variations in input patterns, etc.

1.4.10 Watershed segmentation

The watershed algorithm is an image processing segmentation algorithm that splits an image into areas, based on the topology of the image. The length of the gradients is interpreted as elevation information. During the successive flooding of the grey value relief, watersheds with adjacent catchments basins are constructed.

The watershed segmentation technique is illustrated in figure below:

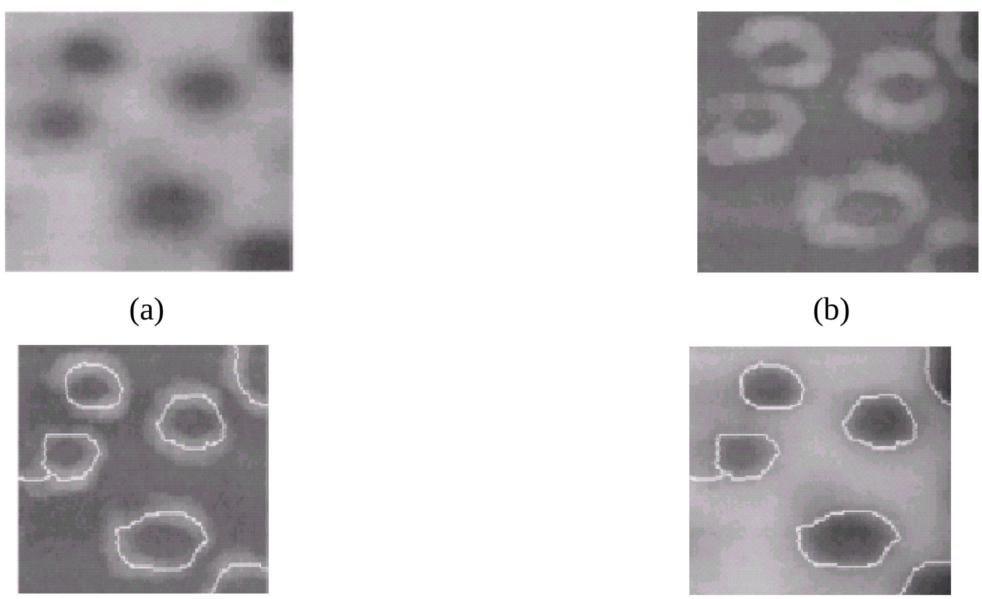

(a) (b) (c) (d)

Figure 1.10: Watershed segmentation (a) Original Image with blob shaped objects, (b) Image Gradient, (c) Watershed Lines, (d) Watershed Lines imposed on Original Image

The flooding process is performed on the gradient image, i.e. the basins should emerge along the edges. Normally this will lead to an over-segmentation of the image, especially for noisy image material, e.g. medical CT data. Either the image must be pre-processed or the regions must be merged on the basis of a similarity criterion afterwards.

A hierarchic watershed transformation converts the result into a graph display (i.e. the neighbor relationships of the segmented regions are determined) and applies further watershed transformations recursively. A problem is that the watersheds will increase in width. The marker based watershed transformation performs flooding starting from specific marker positions which have been either explicitly defined by the user or determined with morphological operators. Interactive watersheds transformations allow to determine include and exclude points to construct artificial watersheds. This can enhance the result of segmentation

1.4.11 Active contour

Active contour, also called snakes, is a framework for delineating an object outline from a possibly noisy 2D image. In contrast to segmenting by thresholding or edge detectors a contour will have an elasticity that is adjusted to the actual application. We can think of an active contour as a snake that bends its body into the edge of the object. An important property of an active contour is the ability to make continuous edges where the edges are weaker. Even if the edge is weak or broken continuous contour can be made.

This framework attempts to minimize an energy associated to the current contour as a sum of an internal and external energy:

$$E_{snake} = E_{internal} + E_{external}$$

- The external energy is supposed to be minimal when the snake is at the object boundary position. The most straightforward approach consists in giving low values when the regularized gradient around the contour position reaches its peak value.
- The internal energy is supposed to be minimal when the snake has a shape which is supposed to be relevant considering the shape of the sought object. The most straightforward approach grants high energy to elongated contours (elastic force) and

to bended/high curvature contours (rigid force), considering the shape should be as regular and smooth as possible.

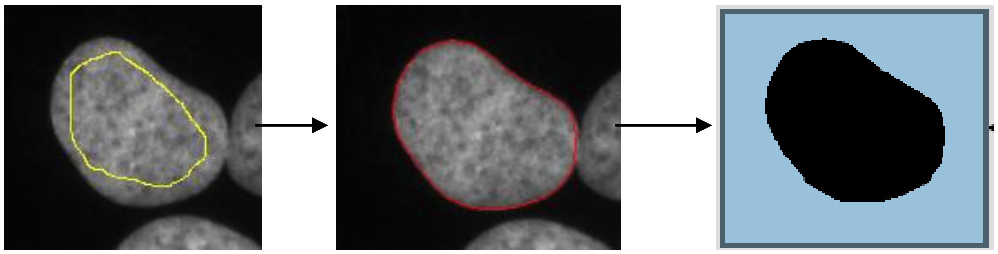

Figure 1.11: Example of active contour

This model is highly popular in computer vision, and led to several developments in 2D and 3D. In two dimensions, the active shape model represents a discrete version of this approach taking advantage of the point distribution model to restrict the shape range to an explicit domain learned from a training set.

1.5 Conclusion

Digital image refers to an image f(x, y) that has been discretized both in spatial coordinates and brightness. A digital image can be considered a matrix whose row and column indices identify a point in the image and the corresponding matrix element value identifies the gray level at that point. Segmentation refers to the process of partitioning a digital image into multiple regions (sets of pixels). The goal of segmentation is to simplify and change the representation of an image into something that is more meaningful and easier to analyze.

CHAPTER 2

REVIEW OF LITERATURE

This chapter provides brief overview of work done in this area.

Lucas Lorenzo et al (1998) proposed a new semi-automatic robust level set based segmentation technique that used both spatial and temporal information. The evolution of level sets was based on a spectral speed function which was a function of the Mahalanobis distance between each pixel's time curve and the time curves of user-determined seed points in the myocardium. A curvature penalty term was included in the evolution of the contours to ensure smoothness of the evolving level sets. Shape information was used to constrain the evolution of the level sets. Shape models were created by using signed distance maps from manually segmented images and performing principal component analysis. Thus the algorithm had the qualities of evolving an active contour both locally, based on image values and curvature, and globally to a maximum a posteriori estimate of the left ventricle shape in order to segment the left ventricle myocardium from DCE cardiac MRI images [1].

Sven Loncaric (2000) proposed a novel technique for 3-D segmentation of abdominal aortic aneurysm from computed tomography (CT) angiography images. The technique was based on 3-D deformable model and utilized the level set algorithm for implementation of the method. The method performed 3-D segmentation of CT images and extracted a 3-D AAA model. Once the 3-D model of AAA was available it was easy to perform all required measurements for appropriate stent graft selection. In this paper, the method used the level-set algorithm instead of the classical active contour. This technique required accurate measurements of the aneurysm for selection of appropriate stent graft shape and size. These measurements were performed by imaging the patient using various medical imaging modalities. A novel 3- D algorithm for abdominal aortic aneurysm segmentation from CT images was presented. The main advantage of the level set algorithm was that it enabled easy segmentation of complex structures [2].

C.F. Westin (1999) presented a novel method for resampling and enhancing image data using multidimensional adaptive filters. This method implemented a 3D affine adaptive filtering scheme and shown how an affine model of the frequency characteristic of the filters can be designed to fit the data geometry and compensate for the anisotropic voxel dimensions normally present in CT data. This process made it possible to obtain a well-tuned frequency characteristic in all directions of the volume, which was of importance since many of the structures of interest had a size close to the signal spacing. Adaptive filtering was used to reduce both the effects of partial volume averaging by resampling the data to a lattice with higher sample density and to reduce the image noise level. Resampling was achieved by constructing filter sets that had subpixel offsets relative to the original sampling lattice. The filters were also frequency corrected for ansisotropic voxel dimensions. The shift and the voxel dimensions were described by an affine transform and provided a model for tuning the filter frequency functions. The method had been evaluated on CT data where the voxels were in general non cubic. The in-plane resolution in CT image volumes was often higher by a factor of 3–10 than the through-plane resolution. The method clearly showed an improvement over conventional resampling techniques such as cubic spline interpolation and sinc interpolation [3].

C. Baillard (2000) presented a strategy for the segmentation of brain from volumetric MR images which integrates 3D segmentation and 3D registration processes. The segmentation process iwas based on the level set formalism. A closed 3D surface propagates towards the desired boundaries through the iterative evolution of a 4D implicit function. In this work, the propagation relies on a robust evolution model including adaptive parameters. These depend on the input data and on statistical distribution models. The main contribution of this paper was the use of an automatic registration method to initialize the surface, as an alternative solution to manual initialization. The registration was achieved through a robust multiresolution and multigrid minimization scheme. This coupling significantly improves the quality of the method, since the segmentation was faster, more reliable and fully automatic. Quantitative and qualitative results on both synthetic and real volumetric brain MR images were presented [4].

M. Droske (2001) presented a multilevel front propagation algorithm for segmentation purposes in three dimensional medical images. Level set techniques deal with non sharp segmentation boundaries. A flexible, interactive modulation of the front speed depending on various boundary and regularization criteria ensures this goal. Efficiency is due to a graded underlying mesh implicitly defined via error or feature indicating values on the cells of the underlying hexahedral grid. A suitable saturation condition ensures an important regularity condition on the resulting adaptive grid. This simplifies the adaptive fast marching method on the compressed data significantly. As an application the segmentation of glioma is considered. Thus the clinician interactively selects a few parameters describing the speed function and a few seed points referring to a single slice of an MRI data set. Then the automatic process of front propagation generates a family of segments corresponding to the evolution of the front in time, from which the clinically selects an appropriate segment covered by the glioma. This selection can be based on a visual evaluation of the propagation on a reference slice using the clinician's expert knowledge. Thus, the overall glioma segmentation turns into an efficient, nearly real time process with intuitive and usefully restricted user interaction [5].

Hongchuan Yu (2001) discussed some questions for applying the level set methods to image segmentation. During image segmentation, it had been found that the level sets function could be changed into a non-distance function with the initial level set function defined as a distance function. This causes some applications in fail, such as Coupled Surfaces Propagation, et al. In addition, the solution existence and uniqueness of the evolving equation in level set method has not been discussed in detail. In this paper; firstly proved that the signed distance function could be preserved to the level set function during the evolution of the level set function through the method. Furthermore, the solution existence and uniqueness of the level set function evolution equations are analyzed in detail under the distance function restriction. And it had been proved that the solutions exist, but not unique. Finally, this conclusion can be validated in the results of implementation on image segmentation [6].

Nathan Moon et al (2002) developed a model-based segmentation method for segmenting head MR image datasets with tumors and infiltrating edema. This was achieved by extending the spatial prior of a statistical normal human brain atlas with individual information derived from the patient's dataset. Thus, combined the statistical geometric prior with image- specification information for both geometry of newly appearing objects, and probability density functions for healthy tissue and pathology. Applications to tumor patients with variable tumor appearance demonstrated that the procedure can handle large variation of tumor size, interior texture, and locality. The method provided a good quality of healthy tissue structures and of the pathology, a requirement for surgical planning or image-guided surgery the segmentation of brain tissue and tumors from three-dimensional magnetic resonance imaging (MRI). The main goal was a high-quality segmentation of healthy tissue and a precise delineation of tumor boundaries. We present an extension to existing expectation maximization (EM) segmentation algorithm that modifies a probabilistic brain atlas with an individual subject's information about tumor location obtained from subtraction of post- and pre-contrast MRI [7].

Nikos Paragios (2002) proposed a new front propagation method to segment MR cardiac images. This framework was based on the Geodesic Active Region Model, refers to a couple propagation of two curves (inner and outer cardiac contours) under the influence of regularity, boundary coupling forces and region based segmentation modules. The boundary information was introduced to the objective function using the gradient vector flow framework while the region information using continuous probability density functions. The defined objective function was minimized using a gradient descent method and the obtained motion equations are implemented using a level set approach. A recently introduced numerical approximation scheme with fast convergence rate and stable behavior was used to implement the level set motion equations. Finally, according to the application the propagations of the level set contours are coupled using their relative distances [8].

Leonid Zhukov Ken (2003) developed a technique that used anisotropic diffusion properties, which did not require eigen value computations. The invariants were used to generate scalar volumes that characterize the total diffusivity and diffusion anisotropy of a DT-MRI scan of a human brain. In this paper, author developed a computational pipeline starting from raw diffusion tensor data, through computation of invariant anisotropy measures to construction of geometric models of the brain structures. This provides an environment for user-controlled 3D segmentation of DT-MRI datasets. Level set approach was used to remove noise from the data and to produce smooth, geometric models. We applied our technique to DT-MRI data of a human subject and build models of the isotropic and strongly anisotropic regions of the brain. Geometric models had been constructed they used to study spatial relationships and quantitatively analyzed to produce the volume and surface area of the segmented regions .Level set modeling and segmentation techniques was applied to the derived scalar volumes and created geometric models of specific brain structures, e.g. the ventricles, corpus callosum and the internal capsul. The geometric models were then used for quantitative analysis, including volume and surface area calculations [9].

Tsai et al (2003) proposed a shape-based approach to curve evolution for the segmentation of medical images containing known object types using Level set segmentation . The author derived a parametric model for an implicit representation of the segmenting curve by applying principal component analysis to a collection of signed distance representations of the training data. . The parameters were then manipulated to minimize an objective function for segmentation. The resulting algorithm was able to handle multidimensional data, can deal with topological changes of the curve, was robust to noise and initial contour placements, and was computationally efficient. At the same time, it avoids the need for point correspondences during the training phase of the algorithm [10].

Hossam Hassan (2004) proposed a shape-based classification technique using the level set approach. A signed distance function was dedicated to describe the model of the tissue of interest. magnetic resonance imaging (MRI) intensity inhomogeneities can be attributed to imperfections in the RF coils or some problems associated with the acquisition sequences. The result was a slowly varying shading artifact over the image that can produce errors with conventional intensity-based classification. The removal of the spatial intensity inhomogeneities from MR images was difficult because the inhomogeneities could change with different MRI acquisition parameters from patient to patient and from slice to slice. Then, a partial differential equation (PDE) was derived to describe the evolution of an observed structure. At each iteration , the observed structure was registered with the prior shape model. The algorithm was used at different levels of noise and intensity inhomogeneities showing a good accuracy [11].

D. Metaxas et al (2004) presented a novel approach towards the goal of automated cardiac segmentation based on variations and improvements of our novel class of deformable models, Metamorphs, which incorporate both texture and shape .The new developments in the formulation of a new class of deformable models, which we term MetaMorphs, and demonstrate the effectiveness of the method in cardiac image segmentation and motion analysis. The formulation of the MetaMorphs naturally integrates both shape and interior texture, and the model deformations are derived from both boundary and region information based on a variational framework. In this paper, in order to address the difficulties in cardiac image segmentation. The author described an automatic and robust way to initialize the metamorph models. A variation of the framework using the parametric curve/surface representation and a hierarchy of global and local deformations was also presented. The author demonstrate the application of the MetaMorph models to segment the epicardium and endocardium surfaces of the RV and LV using CT and MRI-tagged cardiac images. Large-scale textures, such as tag lines in MRI-tagged images, are naturally dealt with in our framework by coupling with the gabor filter banks [12].

Qilong Zhang (2005) presented preliminary efforts towards incorporating manifold learning as a tool to provide additional constraints for segmenting cardiopulmonary images. This approach can be applied to any application domain for which there is a known manifold structure to the data, and may be extended also to other computational shape representation tools (such as snakes). Cardiopulmonary imaging is a key tool in modern diagnostic and interventional medicine. Automated analysis of MRI or ultrasound video was complicated by limitations on the image quality and complicated deformations of the chest cavity created by patient breathing and heart beating. When these were the primary causes of image variation, the video sequence samples a two-dimensional, nonlinear manifold of images. Nonparametric representations of this image manifold can be created using recently developed manifold learning algorithms. For automated analysis tasks that require segmenting many images, this manifold structure provides strong new cues on the shape and deformation of particular regions of interest. This paper developed the theory and algorithms to incorporate manifold constraints within a level set based segmentation algorithm. The author applied the algorithm, based on manifold constraints to the problem of segmenting the left ventricle, and shows the improvement that arises from using the manifold constraints [13].

Y. Chenoune(2005) presented an original method to assess the deformations of the lef ventricular myocardium on cardiac cine-MRI. Because of the wide availability of standard cine-MRI and the mostly automated analytic process, this was a new concept that had a great potential for improved clinical applicability of the quantitative assessment of myocardial strain. To segment the images, the standard method of level set was modified by introducing an additional region-based constraint to the traditional evolution equation. First, a segmentation process, based on a level set method was directly applied on a 2DCt dataset to detect endocardial contours. Second, the successive segmented contours are matched using a procedure of global alignment, followed by a morphing process based on a level set approach. Finally, local measurements of myocardial deformations were derived from the previously determined matched contours. Except for the initialization of the segmentation, which could be reduced to placing one point in the left ventricular cavity on one image of the sequence, the entire procedure was fully automated and provides accurate assessment of myocardial deformation throughout the entire cardiac cycle. The author demonstrated the robustness of this novel method of assessing cardiac deformation that was readily available for routine clinical examinations..This could be tested to estimate tissue. Deformation at mid-wall and within outer myocardial layers (epicardial layers). Also, this would afford the assessment of other parameters of myocardial deformation such as radial thickening and principal strains (E1,E2).The validation step is realized by comparing our results to the measurements achieved on the same patients by an expert using the semi-automated HARP reference method on tagged MR images [14].

Chunming Li (2005) present a new variational formulation for geometric active contours that forces the level set function to be close to a signed distance function, and therefore completely eliminates the need of the costly re-initialization procedure. Our variational formulation consists of an internal energy term that penalizes the deviation of the level set function from a signed distance function, and an external energy term that drives the motion of the zero level set toward the desired image features, such as object boundaries. The resulting evolution of the level set function is the gradient flow that minimizes the overall energy functional [15].

Seongjai Kim (2005) concerned with a level set segmentation algorithm for medical imagery. Due to difficulties such as noise and unclear edges, it was often challenging to obtain a reliable segmentation for medical images. We have considered an efficient and reliable algorithm for PDE-based segmentation. A hybrid model has been suggested combining a gradient-based model and the level set formulation of the Mumford-Shah minimization. We have introduced a linearized alternating direction implicit (ADI) method for efficient time integration and an initialization technique for a fast evolution of the level set function. The method of background subtraction have been adopted and refined in order to improve reliability of the model .For a fast convergence, we also suggest effective initialization strategies for the level set function [16].

R. Manniesing (2006) presented for cerebral vascular tree segmentation from computed tomography angiography (CTA) data. The method started with bone masking by registering a contrast enhanced scan with a low-dose mask scan in which the bone has been segmented. Then an estimate of the background and vessel intensity distributions was made based on the intensity histogram which was used to steer the level set to capture the vessel boundaries. The relevant parameters of the level set evolution are optimized using a training set. The method was validated by a diameter quantification study which was carried out on phantom data, representing ground truth, and 10 patient data sets. The results were compared to manually obtained measurements by two expert observers. In the phantom study, the method achieved similar accuracy as the observers, but was unbiased whereas the observers were biased, i.e., the results are 0.00 ± 0.23 vs. -0.32 ± 0.23 mm. Also, the method's reproducibility was slightly better than the inter-and intra-observer variability. In the patient study, the method was in agreement with the observers and also, the method's reproducibility -0.04 ± 0.17 mm was similar to the inter-observer variability 0.06 ± 0.17 mm. Since the method achieved comparable accuracy and reproducibility as the observers, and since the method achieved better performance than the observers with respect to ground truth.The author concluded that the level set based vessel segmentation was a promising method for automated and accurate CTA diameter quantification [17].

Seong-Jae Lim (2006) proposed a new approach to automatic segmentation of the liver for volume measurement in sequential CT images. This method analyzed the intensity distribution of several abdominal CT samples and exploits priori knowledge, such as CT numbers and location of the liver to identify coherent regions that correspond to the liver. The proposed scheme utilizes recursively morphological filter with region-labeling and clustering to detect the search range and to generate the initial liver contour. In this search range, liver contour was defomed using the labeling-based search algorithm following pattern features of the liver contour. Lastly, volume measurement is automatically performed on the segmented liver regions. The experimental measurement of area and volume was compared with those using manual tracing method as a gold standard by the radiological doctors, and demonstrates that this algorithm was effective for automatic segmentation and volume measurement method of the liver [18].

Shaojun Liu(2006) presented a new level set based solution for automatic medical image segmentation investigate the intensity distribution of these organic structures, and propose a calibrating mechanism to automatically weight image intensity and gradient information in the level set speed function. Level set methods using image intensity or gradient information alone can not generate satisfying segmentation on some complex organic structures, such as lung bronchia or nodules. Intensity distribution based level set method only give instable segmentation results on low-intensity medical structures, due to instable estimation of intensity distribution. Using gradient information to calibrate the intensity distribution based segmentation results. The proposed method tolerates estimation errors of intensity distribution and detects object boundaries whose gradient is low. It filters out some noise and preserves object boundaries with low gradient the proposed method gives stable and accurate segmentation results on public lung image data [19].

Qilong Zhang et al (2006) developed theory and algorithms to incorporate image manifold constraints in a level set segmentation algorithm. This provides a framework to simultaneously segment every image of data sets that vary due to two degrees of freedom such as cardiopulmonary MR images which deform due to patient breathing and heartbeats. We derive two formulations: a 4D level set which loosely couples the level set function between neighbors in the 2D image manifold and a multilayer level set function which uses different levels of the level set function to represent shapes that shrink or grow. We characterize the set of shape manifolds that the multilayer level set function can represent, and derive the evolution equations for both frameworks. We offer results of segmenting the left ventricle in cardiopulmonary MRI; by automatically discovering the 2D manifold structure of the image set then simultaneously segmenting every frame. Both extensions improve on frame-by-frame approaches, and a comparison of the results offers insight into their strengths and weaknesses [20].

Elsa Angelini et al (2006) presented a new homogeneity measure for variation segmentation with multiple level set functions. We proposed a modification of the homogeneity metric used in a multi-phase level set segmentation framework for the segmentation of cortical brain structures. The segmentation method was able to handle multiple MRI data sets without any a priori information and with a common setup We tested in two series of experiments the performance of this new homogeneity force at converging to appropriate partitioning of brain MRI data sets, over a large range of image spatial resolution and image quality, in terms of tissue homogeneity and contrast [21].

Xujia Qin(2007) combined the advantages of Canny operator which can orient the boundary accurately and the idea that Level set method continuously evolves the boundary in image space. The segmentation and extraction of tissues and organs were fundamental work in 3D reconstruction and visualization of medical images. Considering the features of virtual human images, a Canny operator based Level set algorithm and the analytic expression of Level set equation was deduced. Canny operator overcomes the disadvantages of tradition edge detection operators, such as Roberts’s operator, Sobel operator, Prewitt operator and Laplacian operator. It can detect almost all edges, and is one of the best edge detection algorithms. So, we can produce the rough initial contours with Canny operator at first. With initial contours, segment the slice of an by Level Set theory [22].

D. R. Bathula1 (2007) presented a level set based clustering technique to detect activation regions from functional brain images using contextual information. Our approach relies on the idea that voxels within a functional region have similar temporal behavior. Using a level set formulation; a two-dimensional curve is evolved with a speed proportional to a similarity measure between the fMRI signals of voxels lying on the curve and their neighbors in the direction of propagation. The correlation coefficient is used to quantify similarity in time series of adjacent voxels. Simulation results from synthetic images demonstrate that using spatio-temporal contextual information provides better segmentation than a context free, voxel-wise technique. The advantage of clustering using level set approach over voxel-wise thresholding in terms of its ability to (a) reduce false positive and false negative activations and (b) recover activation from significantly reduced time courses .Improvements to the similarity metric and algorithm implementation are also being investigated Results from a real fMRI experiment using auditory stimulation are also presented [23].

Jeongjin Lee (2007) proposed a fast and accurate liver segmentation method from contrast-enhanced computed tomography (CT) images. The two-step seeded region growing (SRG) onto level-set speed images to define an approximate initial liver boundary. The first SRG efficiently divides a CT image into a set of discrete objects based on the gradient information and connectivity. The second SRG detects the objects belonging to the liver based on a 2.5-dimensional shape propagation, which models the segmented liver boundary of the slice immediately above or below the current slice by points being narrow-band, or local maxima of distance from the boundary. With such optimal estimation of the initial liver boundary, the method decreases the computation time by minimizing level-set propagation, which converges at the optimal position within a fixed iteration number. Level-set utilized speed images that have been generally used for level-set propagation to detect the initial liver boundary with the additional help of computationally inexpensive steps, which improves computational efficiency. Finally, a rolling ball algorithm is applied to refine the liver boundary more accurately. This method was validated on 20 sets of abdominal CT scans and the results were compared with the manually segmented result. The average absolute volume error was 1.25 ± 0.70%. The average processing time for segmenting one slice was 3.35 s, which is over 15 times faster than manual segmentation or the previously proposed technique. This method could be used for liver transplantation planning, which requires a fast and accurate measurement of liver volume [24].

Gunnar Lathen(2008) presented an approach for segmenting blood vessels using multi-scale integration of local phase combined with level set propagation. Level set propagation with local phase information to capture the boundaries of vessels. The basic notion was that local phase, extracted using quadrature filters, allows to distinguish between lines and edges in an image. Noting that vessels appear either as lines or edge pairs, integrate multiple scales and capture information about vessels of varying width. The outcome was a "global" phase which can be used to drive a contour robustly towards the vessel edges. Promising results was showed in 2D and 3D. Comparison with a related method gave similar or even better results and at a computational cost several orders of magnitude less. Even with very sparse initializations, our method captures a large portion of the vessel tree [25].

Peder C. Pedersen (2008) evaluated the segmentation which was performed directly in 3D using the level set method, and the level set function was manually initialized. Balloon, curvature, and advection forces were applied to the propagating surface to minimize the energy function of the evolving surface. Relative to other segmentation methods, the level set segmentation yielded a smoother and more realistic looking segmented surface. The accuracy of the level set-based 3 segmentation is influenced by several parameters. Most dramatically is the influence of the complexity of the shape. A global set of level set parameters were chosen for the three categories of images to be segmented. The segmentation performances when the level set parameters were optimized for each image category [26].

Qiangjun Xie et al. (2008) developed an improved level set segmentation method to extract the liver from the abdomen CT image. His region-based level-set approach had many advantages over the conventional active contour models. First, he reduced the real CT image by preprocessing and obtained much smoother contour by adding a signed distance preserving term also speeds up the segmentation process significantly. Second, he obtained accurate extracted liver image by morphological filters. Therefore, the algorithm can be applied to detect the internal malignant structure of liver image. Third, it had better robustness to the presence of weak boundaries and strong noise. This method gives automatic, accurate and much better robustness of organ segmentation under the complex background, by combining other better techniques [27].

Jakub Kratky (2008) proposed a novel fast level set method because of its high computational efficiency, while preserved all advantages of traditional level set methods. His task was to segment bones from 3D CT and MRI images for construction of 3D computer bone models for biomechanical bone analysis. He had presented a novel implementation of the fast level set segmentation algorithm which works on both CT and MRI image modalities with promising results. The algorithm was extended to 3D where the speed advantage over classical level set segmentation were even more pronounced and segmented a CT image of 512 × 512 × 125 in less than 20 s by this method. It was approximately two orders of magnitude faster than standard narrow band algorithms. He also showed high ability of the fast level set algorithm to solve complex segmentation problems [28].

S. Randrianarisolo (2008) presented a method for the assessment of cardiac deformation from standard cine-MRI without requiring tagged MR images.. Firstly, a level set segmentation process is directly applied on a pseudovolumic 2D+t set of images to detect both endocardial and epicardial boundaries. Then the successive contours are matched using an original procedure that consists in an alignment followed by a morphing process. From the matched contours, we deduced an initial velocity of the contour points that will be used in a Thin-Plate Splines approximation method for estimating of the velocity flow on the complete myocardial structure. Finally, local measurements of ventricular deformations are derived from the velocity flow. The validation of the method is performed both mathematically and by comparing the measurements to those obtained on the same patients with the Harmonic Phase reference (HARP) method applied on matched tagged MR images. Our method presents three main advantages. Firstly, it exploits standard untagged cine-MRI, secondly it provides an analysis of the cardiac contraction over an entire cardiac cycle and thirdly, all methods used in this paper are fully and easily extensible in 3D+t [29].

Laurent Massoptier(2008) presented a new method and corresponding algorithm for fast segmentation of the liver and its internal lesions from CT scans.It provided accurate knowledge of the liver structure, including liver surface and lesion localization, is usually required in treatments such as liver tumor ablations and/or radiotherapy. No interaction between the user and analysis system was required for initialization since the algorithm was fully automatic. A statistical model-based approach was created to distinguish hepatic tissue from other abdominal organs. It was combined to an active contour technique using gradient vector flow in order to obtain a smoother and more natural liver surface segmentation. Thereafter, automatic classification was performed to isolate hepatic lesions from liver parenchyma. Twenty-one datasets, presenting different anatomical and pathological situations, have been processed and analyzed. Special focus had been driven to the resulting processing time together with quality assessment. This method allowed robust and efficient liver and lesion segmentations very close to the ground truth, in a relatively short processing time (average of 11.4 s for a 512×512-pixel slice). A volume overlap of 94.2% and an accuracy of 3.7 mm were achieved for liver surface segmentation. Sensitivity and specificity for tumor lesion detection were 82.6% and 87.5%, respectively [30].

Chen G (2009) proposed a implicit contour extraction methods, such as level set methods (LSMs) and active contours, were often used to segment livers, the results were not always satisfactory due to the presence of artifacts and low-gradient response on the liver boundary. A novel multiple-initialization LSM approach was proposed to overcome the leakage and over-segmentation problems in segmenting the liver region from MRIs . An automated liver perfusion analysis method was also proposed to automatically conclude liver perfusion curves and compensate for patient respiration .The multiple-initialization curves were first evolved separately using the fast marching methods and Level set methods, which were then combined with a convex hull algorithm to obtain a rough liver contour. Finally, the contour was evolved again using global level set smoothing to determine a precise liver boundary. The segmentation method had been tested on 12 series of 2-D abdominal MRIs, where the results revealed that the proposed method had the potential to segment the liver region quickly and accurately even from images with more artifacts and lower gradient responses on the boundaries. The accuracy of the proposed method was significantly improved from one of the traditional LSMs [31].

CHAPTER 3
BIOMEDICAL IMAGING

3.1 Introduction

The term image refers to a two-dimensional light intensity f(x, y). Where x and y denote spatial coordinates and the value of f at any point (x, y) is proportional to the brightness (or gray level) of the image at that point. Medical imaging refers to the techniques and processes used to create images of the human body or parts for clinical purposes, that is, medical procedures seeking to reveal, diagnose or examine disease or medical science, including the study of normal anatomy and function

3.2 Digital Images

A digital image is a representation of a two-dimensional image using ones and zeros. The digital image contains a fixed number of rows and columns of pixels. Pixels are the smallest individual element in an image, holding quantized values that represent the brightness of a given color at any specific point. Digital images can be created by a variety of input devices and techniques, such as digital cameras, scanners, coordinate-measuring machines, seismographic profiling, airborne radar, and more.

3.2.1 Types of digital Images

Some of the types of digital images are:

1. Binary image:

This is a digital image that has only two possible values for each pixel. The two colors used for a binary image are black and white though any two colors can be used. The color used for the object(s) in the image is the foreground color while the rest of the image is the background color. Binary images are also called bi-level or two-level. This means that each pixel is stored as a single bit (0 or 1). Binary images often arise in digital image processing as masks or as the result of certain operations such as segmentation, thresholding, and dithering.

2. Grayscale image:

Grayscale digital image is an image in which the value of each pixel is a single sample, that is, it carries only intensity information. Images of this type, also known as black-and-white, are composed exclusively of shades of gray, varying from black at the weakest intensity to white at the strongest. These images with only the two colors black and white. Grayscale images have many shades of gray in between. Grayscale images are also called monochromatic, denoting the absence of any chromatic variation. Grayscale images are often the result of measuring the intensity of light at each pixel in a single band of the electromagnetic spectrum (e.g. infrared, visible light, ultraviolet, etc.)

3. Colour image

A color image is a digital image that includes color information for each pixel. It is necessary to provide three samples for each pixel, which are interpreted as coordinates in some color space. The RGB color spaces is commonly used in computer displays, but other spaces such as YCbCr, HSV, and are often used in other contexts. Some widely used image file formats and graphics cards may use only 8 bits per pixel, i.e. only 256 different colors, or 2–3 bits per channel.

3.3 Medical Imaging

Medical imaging refers to the techniques and processes used to create images of the human body or parts for clinical purposes, that is, medical procedures seeking to reveal, diagnose or examine disease or medical science, including the study of normal anatomy and function. As a discipline and in its widest sense, it is part of biological imaging and incorporates radiology in the wider sense, radiological sciences, endoscopy, (medical) thermography, medical photography and microscopy (e.g. for human pathological investigations).

As a field of scientific investigation, medical imaging constitutes a sub-discipline of biomedical engineering, medical physics or medicine depending on the context: Research and development in the area of instrumentation, image acquisition (e.g. radiography), modelling and quantification are usually the preserve of biomedical engineering, medical physics and computer science; Research into the application and interpretation of medical images is usually the preserve of radiology and the medical sub-discipline relevant to medical condition or area of medical science (neuroscience, cardiology, psychiatry, psychology, etc) under investigation. Many of the techniques developed for medical imaging also have scientific and industrial applications.

Medical imaging is often perceived to designate the set of techniques that noninvasively produce images of the internal aspect of the body. In this restricted sense, medical imaging can be seen as the solution of mathematical inverse problems. This means that cause (the properties of living tissue) is inferred from effect (the observed signal). In the case of ultrasonography the probe consists of ultrasonic pressure waves and echoes inside the tissue show the internal structure. In the case of projection radiography, the probe is X-ray radiation which is absorbed at different rates in different tissue types such as bone, muscle and fat.

3.3.1 Medical imaging techniques

Some of the medical imaging techniques are:

3.3.1.1 Electron microscopy

The electron microscope is a microscope that can magnify very small details with high resolving power due to the use of electrons as the source of illumination, magnifying at levels up to 2,000,000 times.

3.3.1.2 Radiographic

Two forms of radiographic images are in use in medical imaging; projection radiography and fluoroscopy, with latter useful for intraoperative and catheter guidance. These 2D techniques are still in wide use despite the advance of 3D tomography due to the low cost, high resolution, and depending on application, lower radiation dosages. This imaging modality utilizes a wide beam of x rays for image acquisition.

- Fluoroscopy produces real-time images of internal structures of the body in a similar fashion to radiography, but employs a constant input of x-rays, at a lower dose rate. Contrast media, such as barium, iodine, and air are used to visualize internal organs as they work. Fluoroscopy is also used in image-guided procedures when constant feedback during a procedure is required. An image receptor is required to convert the radiation into an image after it has passed through the area of interest. Early on this was a fluorescing screen, which gave way to an Image Amplifier (IA) which was a large vacuum tube that had the receiving end coated with cesium iodide, and a mirror at the opposite end. Eventually the mirror was replaced with a TV camera.

- Projectional radiographs, more commonly known as x-rays, are often used to determine the type and extent of a fracture as well as for detecting pathological changes in the lungs. With the use of radio-opaque contrast media, such as barium, they can also be used to visualize the structure of the stomach and intestines - this can help diagnose ulcers or certain types of colon cancer.

3.3.1.3 Magnetic resonance imaging (MRI)

A magnetic resonance imaging instrument (MRI scanner), or "nuclear magnetic resonance (NMR) imaging" scanner as it was originally known, uses powerful magnets to polarise and excite hydrogen nuclei (single proton) in water molecules in human tissue, producing a detectable signal which is spatially encoded, resulting in images of the body. MRI uses three electromagnetic fields: a very strong (on the order of units of teslas) static magnetic field to polarize the hydrogen nuclei, called the static field; a weaker time-varying (on the order of 1 kHz) field(s) for spatial encoding, called the gradient field(s); and a weak radio-frequency (RF) field for manipulation of the hydrogen nuclei to produce measurable signals, collected through an RF antenna.

3.3.1.4 Nuclear medicine

Nuclear medicine on a whole encompasses both the diagnosis and treatment of disease using nuclear properties. In imaging the energetic photons emitted from radioactive nuclei are used for enhancing and viewing various pathologies.

- **Gamma cameras** are used in nuclear medicine to detect regions of biological activity that are often associated with diseases. A short lived isotope, ^{123}I are more readily absorbed by biologically active regions of the body, such as tumors or fracture points in bones.

- **Positron emission tomography (PET)** is primarily used to detect diseases of the brain and heart. Similarly to nuclear medicine, a short-lived isotope, such as ^{18}F, is incorporated into a substance used by the body such as glucose which is absorbed by the tumor of interest. PET scans are often viewed alongside computed tomography scans, which can be performed on the same equipment without moving the patient. This allows the tumors detected by the PET scan to be viewed next to the rest of the patient's anatomy detected by the CT scan. Another 3D tomographic technique is SPECT but uses gamma camera like method for reconstruction.

3.3.1.5. Photoacoustic imaging

Photoacoustic imaging is a recently developed hybrid biomedical imaging modality based on the photoacoustic effect. It combines the advantages of optical absorption contrast with ultrasonic spatial resolution for deep imaging in (optical) diffusive or quasi-diffusive regime. Recent studies have shown that photoacoustic imaging can be used in vivo for tumor angiogenesis monitoring, blood oxygenation mapping, functional brain imaging, and skin melanoma detection, etc.

3.3.1.6. Tomography

Tomography is the method of imaging a single plane, or slice, of an object resulting in a tomogram. There are several forms of tomography:

- **Linear tomography**: This is the most basic form of tomography. The X-ray tube moved from point "A" to point "B" above the patient, while the cassette holder (or "bucky") moves simultaneously under the patient from point "B" to point "A." The fulcrum, or pivot point, is set to the area of interest. In this manner, the points above and below the focal plane are blurred out, just as the background is blurred when panning a camera during exposure. No longer carried out and replaced by computed tomography.
- **Poly tomography**: This was a complex form of tomography. With this technique, a number of geometrical movements were programmed, such as hypocycloidic,

circular, figure 8, and elliptical. Philips Medical Systems produced one such device called the 'Polytome.' This unit was still in use into the 1990s, as its resulting images for small or difficult physiology, such as the inner ear, was still difficult to image with CTs at that time. As the resolution of CTs got better, this procedure was taken over by the CT.

- **Zonography:** This is a variant of linear tomography, where a limited arc of movement is used. It is still used in some centres for visualizing the kidney during an intravenous urogram (IVU).
- **Orthopantomography (OPT or OPG):** The only common tomographic examination in use. This makes use of a complex movement to allow the radiographic examination of the mandible, as if it were a flat bone. It is often referred to as a "Panorex", but this is incorrect, as it is a trademark of a specific company's equipment
- **Computed Tomography (CT), or Computed Axial Tomography (CAT):** A CT scan, also known as a CAT scan, is a helical tomography (latest generation), which traditionally produces a 2D image of the structures in a thin section of the body. It uses X-rays. It has a greater ionizing radiation dose burden than projection radiography; repeated scans must be limited to avoid health effects.

3.3.1.7. Ultrasound

Medical ultrasonography uses high frequency broadband sound waves in the megahertz range that are reflected by tissue to varying degrees to produce (up to 3D) images. This is commonly associated with imaging the fetus in pregnant women. Uses of ultrasound are much broader, however. Other important uses include imaging the abdominal organs, heart, breast, muscles, tendons, arteries and veins. While it may provide less anatomical detail than techniques such as CT or MRI, it has several advantages which make it ideal in numerous situations, in particular that it studies the function of moving structures in real-time, emits no ionizing radiation, and contains speckle that can be used in elastography. It is very safe to use and does not appear to cause any adverse effects, although information on this is not well documented. It is also relatively inexpensive and quick to perform. Ultrasound scanners can be taken to critically ill patients in intensive care units, avoiding the danger caused while moving the patient to the radiology department. The real time moving image obtained can be used to guide drainage and biopsy procedures. Doppler capabilities on modern scanners allow the blood flow in arteries and veins to be assessed.

3.4 X-ray

X-rays is a form of electromagnetic radiation. It has a wavelength in the range of 10 to 0.01 nanometers, corresponding to frequencies in the range 30 petahertz to 30 exahertz (3×10^{16} Hz to 3×10^{19} Hz) and energies in the range 120 eV to 120 keV. They are shorter in wavelength than UV rays. They are primarily used for diagnostic radiography and crystallography. The term X-ray is metonymically used to refer to a radiographic image produced using this method, in addition to the method itself. X-rays are a form of ionizing radiation and as such can be dangerous. X-rays span 3 decades in wavelength, frequency and energy. From about 0.12 to 12 keV they are classified as soft X-rays, and from about 12 to 120 keV as hard X-rays, due to their penetrating abilities.

An X-ray machine utilizes electromagnetic radiation to produce an image of an object, usually with the purpose of visualizing something located below the object's surface. The machine is made up of an X-ray source or X-ray tube, an x-ray detection system, and positioning hardware to align these two components with the object to be imaged.

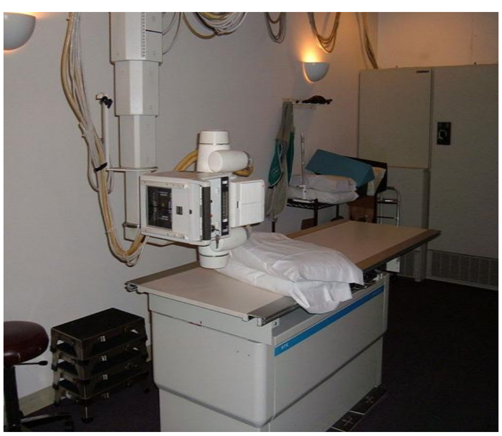

Figure3.1: X-ray machine with table

Figure 3.2: Mobile medical X-ray machine

3.4.1 Working of X-ray machine

An X-ray machine is essentially a camera. Instead of visible light, however, it uses X-rays to expose the film. X-rays are like light in that they are electromagnetic waves, but they are more energetic so they can penetrate many materials to varying degrees. When the X-rays hit the film, they expose it just as light would. Since bone, fat, muscle, tumors and other masses all absorb X-rays at different levels, the image on the film lets you see different (distinct) structures inside the body because of the different levels of exposure on the film

An X-ray imaging system consists of an X-ray source or generator, and an image detection system which can either be comprised of film (analog technology) or a digital capture system.

- **X-ray Sources**

In the typical X-ray source of less than 450 kV, X-ray photons are produced by an electron beam striking a target. The electrons that make up the beam are emitted from a heated cathode filament. The electrons are then focused and accelerated towards an angled anode target. The point where the electron beam strikes the target is called the focal spot. Most of the kinetic energy contained in the electron beam is converted to heat, but around 10% of the energy is converted into X-ray photons, the excess heat is dissipated via a heat sink. At the focal spot, X-ray photons are emitted at 180deg from the target surface, the highest intensity being around 60deg to 90deg there is a small round window in the X-ray tube directly above the angled target. This window allows the X-ray to exit the tube with little attenuation while maintaining a vacuum seal required for the X-ray tube operation. X-ray machines work by applying controlled voltage, current, and time to the X-ray tube, which results in a beam of X-rays. The beam is projected on matter. Some of the X-ray beam will pass through the object, while some are reflected. The resulting pattern of the radiation is then ultimately detected by a detection medium including rare earth screens (which surround photographic film), semiconductor detectors, or X-ray image intensifiers.

- **X-Ray Detection**

In healthcare applications in particular, the x-ray detection system rarely consists of the detection medium. For example, a typical stationary radiographic x-ray machine also includes an ion chamber and grid. The ion chamber is basically a hollow plate located between the detection medium and the object being imaged. It determines the level of exposure by measuring the amount of x-rays that have passed through the electrically charged, gas-filled gap inside the plate. This allows for minimization of patient radiation exposure by both ensuring that an image is not underdeveloped to the point the exam needs to be repeated and ensuring that more radiation than needed is not applied. The grid is usually located between the ion chamber and object and consists of several lead slats stacked next to each other (resembling open window blinds). In this manner, the grid allows straight x-rays to pass through to the detection medium but absorbs reflected x-rays. This improves image quality by preventing reflected (non-diagnostic) x-rays from reaching the detection medium allowing for lower exam doses overall. Images taken with such devices are known as X-ray photographs or radiographs.

3.4.2 Applications

X-ray technology is used in health care for visualizing bone structures and other dense tissues such as tumors. Non-medical applications include security and material analysis. (Xerographic Radiation)

1. Medicine

The two main fields in which x-ray machines are used in medicine are radiography and dentistry.

Radiography is used for fast, highly penetrating images, and is usually used in areas with high bone content. Some forms of radiography include:

- Orthopantomogram — a panoramic x-ray of the jaw showing all the teeth at once
- Mammography — x-rays of breast tissue
- Tomography — x-ray imaging in sections
- Radiotherapy — the use of x-ray radiation to treat malignant cancer cells, a non imaging application.

Fluoroscopy is used in cases where real-time visualization is necessary. Some medical applications of fluorography include:

- Angiography — used to examine blood vessels in real time

- Barium enema — a procedure used to examine problems of the colon and lower gastrointestinal tract
- Barium swallow — similar to a barium enema, but used to examine the upper gastrointestinal tract
- Biopsy — the removal of tissue for examination

X-rays are highly penetrating, ionizing radiation; therefore X-ray machines are used to take pictures of dense tissues such as bones and teeth. This is because bones absorb the radiation more than the less dense soft tissue. X-rays from a source pass through the body and onto a photographic cassette. Areas where radiation is absorbed show up as lighter shades of grey (closer to white). This can be used to diagnose broken or fractured bones. In fluoroscopy, imaging of the digestive tract is done with the help of a radio contrast agent such as barium sulfate, which is opaque to X-rays.

2. Security

X-ray machines are used to screen objects non-invasively. Luggage at airports and student baggage at many schools are examined for possible weapons, including bombs. These machines are very low dose and safe to be around. The main parts of an X-ray Baggage Inspection System are the generator used to generate x-rays, the detector to detect radiation after passing through the baggage, signal processor unit (usually a PC) to process the incoming signal from the detector, and a conveyor system for moving baggage into the system.

Figure 3.3:X-ray machine for security

3.5 Computed Tomography (CT)

Computed tomography (CT) is a medical imaging method employing tomography. Digital geometry processing is used to generate a three-dimensional image of the inside of an object from a large series of two-dimensional X-ray images taken around a single axis of rotation .CT produces a volume of data which can be manipulated, through a process known as" windowing. In order to demonstrate various bodily structures based on their ability to block the X-ray/Röntgen beam. Although historically the images generated were in the axial or transverse plane, orthogonal to the long axis of the body, modern scanners allow this volume of data to be reformatted in various planes or even as volumetric (3D) representations of structures. Although most common in medicine, CT is also used in other fields, such as nondestructive materials testing and also uses to study biological and paleontological specimens.

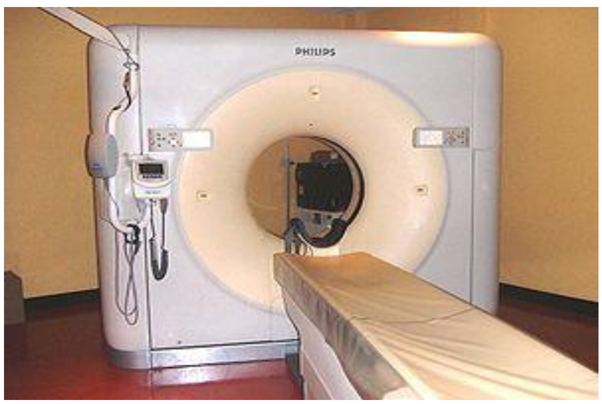

Figure 3.4: A multislice CT scanner

3.5.1 Working of CT scanner

The CT scanner consists of a couch upon which the patient is placed and a circular gantry through which the couch with patient is passed. Within the gantry is a rotating ring with an X-ray source opposed to a linear array of detectors. A typical CT scan machine is shown in Figur2.1.The X-ray source is collimated so that the X-rays form a flat fan beam with a thickness determined by the user. During the acquisition of a "slice" of data, the source detector ring is rotated around the patient.

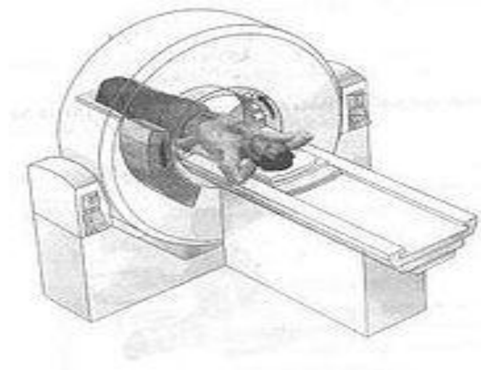

Figure 3.5: CT scanner

The raw output from the detector array is back projected to form an image of the slice of the body. The couch is moved and then another slice is obtained.

The output from a CT scanner is a series of trans axial slices of the patient. Each slice represents a slab of the patients' body with a thickness set by the collimation for the slice (typically 1-10mm). For most CT scanners each slab has 512 by 512 pixels. The size of a pixel can be varied within certain limits (generally 0.5 to 2 mm).

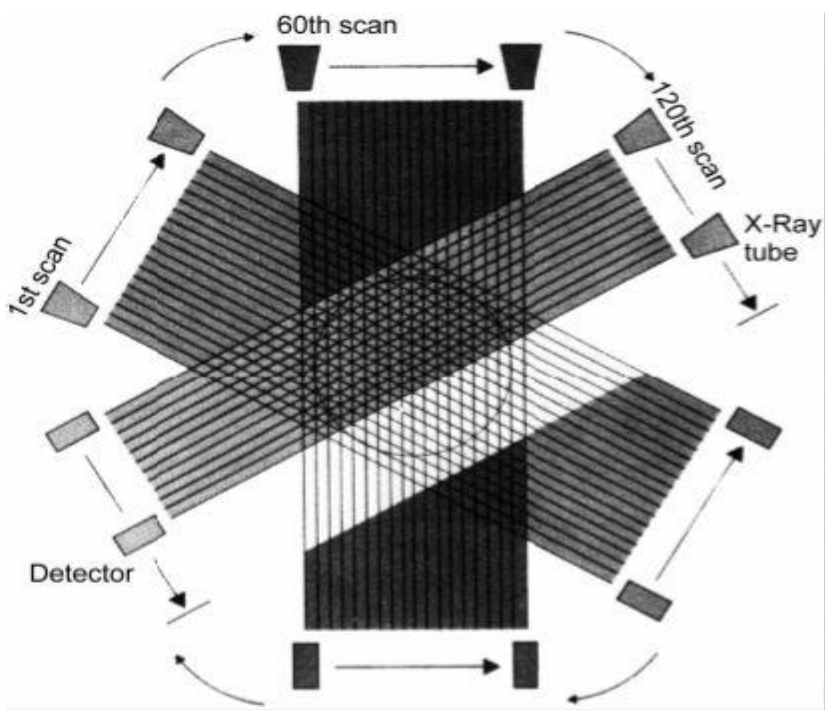

Figure 3.6: Various scans at different angles

Generally each slice is spaced such that they are either overlapping or contiguous, though some protocols call for gaps between the slices. Each pixel ideally represents the absorption characteristics of the small volume. Modern CT scanners can generally acquire one slice within 1 to 5 seconds. An entire study of a patient generally represents 30-40 slices, with a study time of 3-15 minutes. The radiation dose from a CT scan is comparable with that of a series of traditional X-rays. This is measured in Hounsfield units (HU). X-ray slice data is generated using an X-ray source that rotates around the object X-ray sensors are positioned on the opposite side of the circle from the X-ray source Figure 3.6 shows various scans at different angles. CT produces a volume of data which can be manipulated, through a process known as windowing, in order to demonstrate various structures based on their ability to block the X-ray beam. A CT scanner uses a series of X-ray beams to build up images of the body in slices. Unlike an X-ray, which sends one beam of radiation through the body, a CT scanner emits a succession of narrow beams as it moves through an arc. This produces a very detailed image that is not possible from x-ray.

A relatively new technique, a spiral CT has improved the speed and accuracy of the scan for many diseases. The X-ray beam takes a continuous spiral path during scanning, gathering continuous data with no gaps between images. A spiral scan can usually be obtained while holding your breath, which allows a scan of the chest to be done in a few seconds.

3.5.2 Advantages of CT scan

The following advantages of the CT scan are:

- CT scan completely eliminates the superimposition of images of structures outside the area of interest.
- In CT scan, the differences between tissues that differ in physical density by less than 1% can be distinguished because the inherent high-contrast resolution of CT.
- The data from a single CT imaging procedure consisting of either multiple contiguous or one helical scan can be viewed as images in the axial, coronal, or sagittal planes, depending on the diagnostic task. This is referred to as multiplanar reformatted imaging.

- CT may be enhanced by use of contrast agents containing elements of a higher atomic number than the surrounding flesh (iodine, barium).
- CT a good tool for examining tissue composed of elements of a relatively higher atomic number than the tissue surrounding them, such as bone and calcifications (calcium based) within the body (carbon based flesh), or of structures (vessels, bowel).
- The development of multi-detector CT scanners with near-isotropic resolution, allows the CT scanner to produce data that can be retrospectively reconstructed in any plane with minimal loss of image quality.
- CT usually is more widely available, faster, much less expensive, and may less likely to require the person to be sedated or anesthetized.

3.5.3 Hazards of CT scan

The following hazards of the CT scan are:

- The radiation from current CT-scan use may cause as many as 1 in 50 future cases of cancer.
- Pregnant women should not have a CT scan, as there is a small risk that X-rays may cause an abnormality to the unborn child. Nursing mothers should wait for 24 hours after contrast material injection before resuming breast-feeding.
- The contrast dye used in CT scans often contains iodine, which can cause an allergic reaction in a few people. Very rarely the dye may cause some kidney damage in people who already have kidney problems.
- Children should have a CT scan only if it is essential for making a diagnosis and should not have repeated CT studies unless absolutely necessary as CT scans of children have been estimated to produce non-negligible increases in the probability of lifetime cancer mortality.

3.5.4 Artifacts

CT is a relatively accurate test; it is liable to produce artifacts, such as the following:

- **Aliasing Artifact or Streaks:**

These appear as dark lines which radiate away from sharp corners. It occurs because it is impossible for the scanner to 'sample' or take enough projections of the object, which is usually metallic. These artifacts are also closely tied to motion during a scan. This type of artifact commonly occurs in head images around the pituitary fossa area.

- **Partial Volume Effect**:

This appears as 'blurring' over sharp edges. It is due to the scanner being unable to differentiate between a small amount of high-density material (e.g. bone) and a larger amount of lower density (e.g. cartilage).. This can be partially overcome by scanning using thinner slices.

- **Ring Artifact:**

Probably the most common mechanical artifact, the image of one or many 'rings' appears within an image. This is usually due to a detector fault.

- **Noise Artifact:**

This appears as graining on the image and is caused by a low signal to noise ratio. This occurs more commonly when a thin slice thickness is used. It can also occur when the power supplied to the X-ray tube is insufficient to penetrate the anatomy.

- **Motion Artifact**:

  This is seen as blurring and/or streaking which is caused by movement of the object Being imaged

- **Windmill:**

Streaking appearances can occur when the detectors intersect the reconstruction plane. This can be reduced with filters or a reduction in pitch.

- **Beam Hardening**:

This can give a 'cupped appearance'. It occurs when there is more attenuation in the center of the object than around the edge. This is easily corrected by filtration and software.

3.6 Magnetic Resonance Imaging (MRI)

Magnetic resonance imaging (MRI) is the newest, and perhaps most versatile, medical imaging technology available. Doctors can get highly refined images of the body's interior without surgery, using MRI. By using strong magnets and pulses of radio waves to manipulate the natural magnetic properties in the body, this technique makes better images of organs and soft tissues than those of other scanning technologies. It is primarily a medical imaging technique most commonly used in radiology to visualize the internal structure and function of the body. MRI provides much greater contrast between the different soft tissues of the body than computed tomography (CT) does, making it especially useful in neurological (brain), musculoskeletal, cardiovascular, and oncological (cancer) imaging

Figure 3.7: Modern clinical MRI scanner

Unlike CT, it uses no ionizing radiation, but uses a powerful magnetic field to align the nuclear magnetization of (usually) hydrogen atoms in water in the body. Radio frequency (RF) fields are used to systematically alter the alignment of this magnetization, causing the hydrogen nuclei to produce a rotating magnetic field detectable by the scanner. This signal can be manipulated by additional magnetic fields to build up enough information to construct an image of the body.

3.6.1 Working of MRI

The body is mainly composed of water molecules which each contain two hydrogen nuclei or protons. When a person goes inside the powerful magnetic field of the scanner these protons align with the direction of the field.A second radio frequency electromagnetic field is then briefly turned on causing the protons to absorb some of its energy. When this field is turned off the protons release this energy at a radio frequency which can be detected by the scanner. The position of protons in the body can be determined by applying additional magnetic fields during the scan which allows an image of the body to be built up. These are created by turning gradients coils on and off which creates the knocking sounds heard during an MR scan.

Diseased tissue, such as tumors, can be detected because the protons in different tissues return to their equilibrium state at different rates. By changing the parameters on the scanner this effect is used to create contrast between different types of body tissue.Contrast agents may be injected intravenously to enhance the appearance of blood vessels, tumors or inflammation. Contrast agents may also be directly injected into a joint in the case of arthrograms, MR images of joints.

3.6.2 MRI scanner construction and operation

The major components of an MRI scanner are a static magnetic field, an RF transmitter and receiver, and three orthogonal, controllable magnetic gradients.

1. Magnet:

The magnet is the largest and most expensive component of the scanner, and the remainder of the scanner is built around it. The strength of the magnet is precision is measured in tesla (T). The straightness of the magnetic lines within the center (or, as it is technically known, the iso-center) of the magnet needs to be near-perfect. This is known as homogeneity. Fluctuations (inhomogeneities in the field strength) within the scan region should be less than three parts per million (3 ppm). Three types of magnets have been used:

- Permanent magnet
- Resistive electromagnet
- Superconducting electromagnet

Magnetic field strength is an important factor in determining image quality. Higher magnetic fields increase signal-to-noise ratio, permitting higher resolution or faster scanning. However, higher field strengths require more costly magnets with higher maintenance costs, and have increased safety concerns. A field strength of 1.0 - 1.5 T is a good compromise between cost and performance for general medical use. However, for certain specialist uses (e.g., brain imaging) higher field strengths are desirable, with some hospitals now using 3.0 T scanners.

2. Radio frequency system:

The radio frequency (RF) transmission system consists of an RF synthesizer, power amplifier and transmitting coil. This is usually built into the body of the scanner. The power of the transmitter is variable, but high-end scanners may have a peak output power of up to 35 kW, and be capable of sustaining average power of 1 kW. The receiver consists of the coil, pre-amplifier and signal processing system. While it is possible to scan using the integrated coil for RF transmission and MR signal reception, if a small region is being imaged, then better image quality (i.e., signal-to-noise ratio) is obtained by using a close-fitting smaller coil. A variety of coils are available which fit closely around parts of the body, e.g., the head, knee, wrist, breast, or internally, e.g., the rectum.

3. Gradients:

Scan speed is dependent on performance of the gradient system. Gradient coils are used to spatially encode the positions of protons by varying the magnetic field linearly across the imaging volume. The Larmor frequency will then vary as a function of position in the x, y and z-axes.

Gradient coils are usually resistive electromagnets powered by sophisticated amplifiers which permit rapid and precise adjustments to their field strength and direction. Typical gradient systems are capable of producing gradients from 20 mT/m to 100 mT/m (i.e., in a 1.5 T magnet, when a maximal z-axis gradient is applied, the field strength may be 1.45 T at one end of a 1 m long bore and 1.55 T at the other[).

3.6.3 Advantages of MRI

The advantages of MRI are:

- MRI is used to distinguish pathologic tissue from normal tissue.

- MRI scan is harmless to the patient. It uses strong magnetic fields and non-ionizing radiation in the radio frequency range. It may not increase the risk of malignancy, especially in a fetus.
- MRI provides comparable resolution with far better contrast resolution (the ability to distinguish the differences between two arbitrarily similar but not identical tissues).
- MRI, on the other hand, uses non-ionizing radio frequency (RF) signals to acquire its images and is best suited for non-calcified tissue, though MR images can also be acquired from bones and teeth
- MRI avoids the use of ionizing radiation, to which the fetus is particularly sensitive. Only MRI recommend to the pregnant women undergo when essential
- MRI is also best suited for cases when a patient is to undergo the exam several times successively in the short term.

3.7 Conclusion

Medical imaging is widely used to diagnosis and biomedical images medical such as X-ray,CT scan, MRI etc. Imaging is generally equated to radiology or "clinical imaging" and the medical practitioner responsible for interpreting the image is a radiologist. Diagnostic radiography designates the technical aspects of medical imaging and in particular the acquisition of medical images.

CHAPTER 4

PROBLEM FORMULATION

4.1 Introduction

There is different segmentation techniques used for images segmentation but in this thesis level set segmentation method is used. This method used to represent the evolving contour using a signed function, where its zero level corresponds to the actual contour. Filtering is used to enhance, smoothens and remove noise from the image. Spatial filtering is mainly used in digital images.

4.2 Level set segmentation

The level set method was initially proposed to track moving interfaces by Osher and Sethian in 1988 and has spread across various imaging domains in the late nineties. It can be used to efficiently address the problem of curve/surface/etc. propagation in an implicit manner. The central idea is represent the evolving contour using a signed function, where its zero level corresponds to the actual contour. Then, according to the motion equation of the contour, one can easily derive a similar flow for the implicit surface that when applied to the zero-level will reflect the propagation of the contour. The existing active contour models can be broadly classified as either parametric active contour model or geometric active contour models according to their representation and implementation. These models are based on curve evolution theory and level set method. The basic idea is to represent contours as the zero level set of an implicit function defined in a higher dimension, usually referred as the level set function, and to evolve the level set function according to a partial differential equation (PDE). This approach presents several advantages over the traditional parametric active contours. First, the contours represented by the level set function may break or merge naturally during the evolution, and the topological changes are thus automatically handled. Second, the level set function always remains a function on a fixed grid, which allows efficient numerical schemes.

Reinitialization, a technique for periodically re-initializing the level set function to a signed distance function during the evolution, has been extensively used as a numerical remedy for maintaining stable curve evolution and ensuring usable results. The level set function is obviously a disagreement between the theory of the level set method and its implementation using re-initialization. These schemes have an undesirable side effect of moving the zero level set away from its original location. It still remains a serious problem as when and how to apply the re-initialization. Our variational energy functional consists of an internal energy term and an external energy term, respectively.

The resulting evolution of the level set function is the gradient flow that minimizes the overall energy functional. Due to the internal energy, the level set function is naturally and automatically kept as an approximate signed distance function during the evolution. Therefore, the re-initialization procedure is completely eliminated.

The variation level set formulation has main advantages over the traditional level set formulations:

- A significantly larger time step can be used for numerically solving the evolution PDE, and therefore speeds up the curve evolution.
- The level set function could be initialized as functions that are computational more efficient to generate than the signed distance function.
- The proposed level set evolution can be implemented using simple finite difference scheme, instead of complex upwind scheme as in traditional level set formulations.
- The variation level set formulation has been applied to both simulated and real images with promising results. It appears to perform robustly in the presence of weak boundaries.

4.2.1 Traditional Level Set Methods

In level set formulation of level-sets, the level-set is denoted by C, are represented by the zero level set.

$$C\ (t) = \{(x, y)\ |\ \emptyset\ (t, x, y) = 0\} \qquad 4.1$$

of a level set function $\emptyset(t, x, y)$. The evolution equation of the level set function $\emptyset$ can be written in the following form:

$$\frac{\partial \emptyset}{\partial t} + F|\nabla\emptyset|=0 \qquad . \qquad 4.2$$

which is called level set equation. The function F is called the speed function. For image segmentation, the function F depends on the image data and the level set function $\emptyset$. In traditional level set methods, the level set function $\emptyset$ can develop shocks, very sharp and/or flat shape during the evolution, which makes further computation highly inaccurate. To avoid these problems, a common numerical scheme is to initialize the function $\emptyset$ as a signed distance function before the evolution, and then "reshape" (or "re-initialize") the function $\emptyset$ to be a signed distance function periodically during the evolution. Indeed, the reinitialization process is crucial and cannot be avoided in using traditional level set methods.

4.2.2 Drawbacks Associated with Re-initialization

Re-initialization has been extensively used as a numerical remedy in traditional level set methods. The standard re-initialization method is to solve the following reinitialization equation:

$$\frac{\partial \emptyset}{\partial t} = \text{sign}\,(\emptyset_0)\,(1-|\,\nabla\emptyset|) \qquad 4.3$$

where $\emptyset_0$ is the function to be re-initialized, and sign($\emptyset$) is the sign function. But problem is there if $\emptyset_0$ is not smooth or $\emptyset_0$ is much steeper on one side of the interface than the other, the zero level set of the resulting function $\emptyset$ can be moved incorrectly from that of the original function. For removing this limitation we use new approach of Variational Level Set Formulation of Curve Evolution without Re-initialization.

The evolving level set function can deviate greatly from its value as signed distance in a small number of iteration steps, especially when the time step is not chosen small enough.So far, re-initialization has been extensively used as a numeric remedy for maintaining stable curve evolution and ensuring desirable results. The re-initialization process can be quite complicated, expensive and have subtle side effects.

4.2.3 Variational level set formulation of curve evolution without re-initialization

The level-set are dynamic curves that move toward the object boundaries. Therefore we define an external energy that can move towards the edges. If I be the image, then edge indicator function (g) is defined by:

$$g = \frac{1}{1+|\nabla G_\sigma * I|^2} \qquad 4.4$$

where G_σ is the Gaussian kernel with standard deviation σ. We define an external energy for a function Ø(x, y) as below:

$$E_{g,}\ \lambda,\ \alpha\ (\emptyset) = \lambda\ L_g\ (\emptyset) + \alpha\ A_g\ (\emptyset) \qquad 4.5$$

where λ > 0 and α are constants, and the terms Lg(Ø) and Ag(Ø) are defined by

$$L_g\ (\emptyset) = \int_\Omega g\varepsilon\ (\emptyset)\ |\nabla\emptyset| dxdy \qquad 4.6$$

And,

$$A_g\ (\emptyset) = \int gH\ (-\emptyset)\ dxdy \qquad 4.7$$

respectively, where ∈ is the unvariate Dirac function, and H is the HZeaviside function. Now, the following total energy functional.

$$E\ (\emptyset) = \mu P\ (\emptyset) + E_{g,\ \lambda},\ \propto\ (\emptyset) \qquad 4.8$$

The external energy Eg, λ, Ø ∝ drives the zero level set towards the object boundaries, while the internal energy μP (Ø) penalizes the deviation of Ø from a signed distance function during its evolution which is give in equation given below:

$$P\ (\emptyset) = \int_\Omega \frac{1}{2}(|\nabla\emptyset|-1)^2 dxdy \qquad 4.9$$

The variational formula derives from the penalize energy equation:

$$E(\emptyset) = \mu . p(\emptyset) + E_m \qquad 4.10$$

where $\mu > 0$ is a parameter controlling the effect of penalizing the deviation of $\emptyset$ from a signed distance function, and E_m ($\emptyset$) is a certain energy that would drive the motion of the zero level curve of $\emptyset$ .The energy functional Ag ($\emptyset$) introduced to speed up curve evolution. The coefficient $\propto$ of Ag can be positive or negative, depending on the relative position of the initial level-set to the object of interest. If the initial level-sets are placed inside the object, the coefficient $\propto$ should take negative value to speed up the expansion of the level-sets. By calculus of variations, the Gateaux derivative of the functional E in can be written as

$$\frac{\partial E}{\partial \emptyset} = -\mu \left[\Delta\emptyset - \mathrm{div}\left(\frac{\nabla\emptyset}{|\nabla\emptyset|}\right)\right] - \lambda\delta(\emptyset)\,\mathrm{div}\left(g\frac{\nabla\emptyset}{|\nabla\emptyset|}\right) - \propto g\varepsilon(\emptyset) \qquad 4.11$$

Where Δ is the Laplacian operator, Therefore, the function $\emptyset$ that minimizes this functional satisfies the Euler-Lagrange equation $\frac{\partial E}{\partial \emptyset} = 0$. The gradient flows of the energy function $\lambda Lg(\emptyset)$ and $\propto Ag(\emptyset)$,are responsible of driving the zero level curve towards the object boundaries.So this new approach of level-sets is tested on medical images like CT, X-Ray and MRI. It shows good result on medical images even on more noisy images. But one problem is there that is we have to make the level-set optimized to the particular image, and if images changes than topology has to change by user itself.

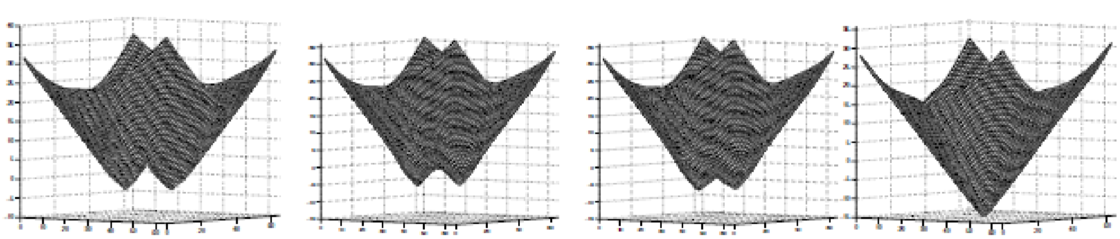

Figure 4.1: Evolution of function $\emptyset$

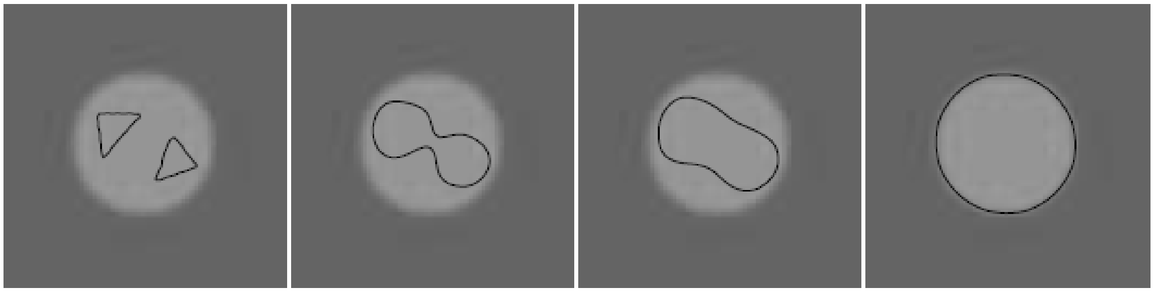

Figure 4.2: Evolution of zero level curve of the corresponding level set function Ø

Example of the level set segmentation on biomedical images:

(a) (b)

Figure 4.3: (a) 2-D MRI image (b) Segmentation of 2-D MRI image

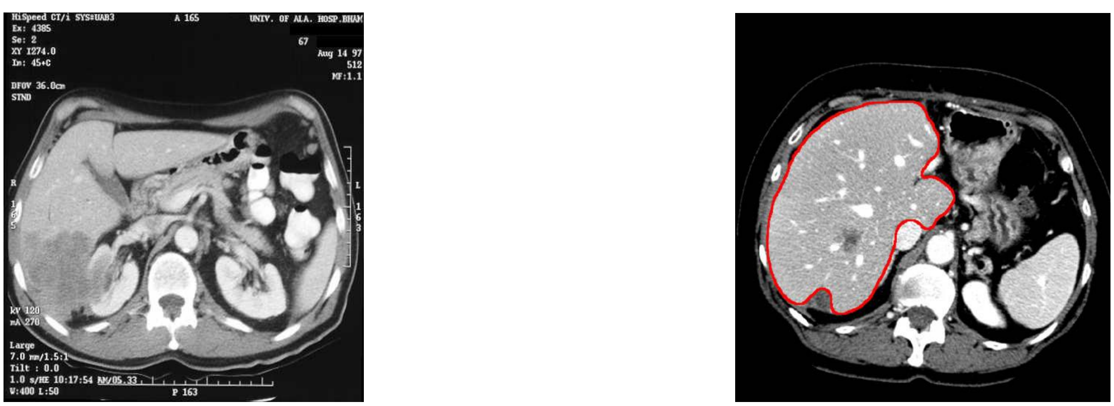

(a) (b)

Figure 4.4: (a) CT image (b) Segmentation of CT image

4.3 Spatial Filtering:

The term spatial filtering is principally associated with digital image processing, although such methods may be applied to almost any type of grid or image. Spatial filtering term is the filtering operations that are performed directly on the pixels of an image. A method of spatially filtering a digital image includes receiving a source digital image including pixels corresponding to one or more different colors; selecting a pixel of interest in the source digital image; calculating two or more noise free pixel estimates for the pixel of interest using pixel values sampled in a local region about the pixel of interest; selecting a final noise free pixel estimate for the pixel of interest from the noise free pixel estimates; and repeating for other pixels in the source digital image to provide a spatially filtered digital image.

4.3.1 Types of Spatial Filtering

1. Linear spatial filtering
2. Non- Linear spatial filtering

4.3.1.1 Linear Filtering

This filtering is based on neighborhood operation and the mechanism of defining m*n neighborhood by sliding the center .This is based on the sliding on computing the sum of products. The linear spatial filtering using function: imfilter and fspecial.

1. Imfilter:

Filtering of images, either by correlation or convolution can be performed using the toolbox function imfilter.. The imfilter function handles data types similarly to the way the image arithmetic functions. The imfilter function computes the value of each output pixel using double-precision, floating-point arithmetic.. If it is an integer data type, imfilter rounds fractional values.

Syntax of imfilter:

G=imfilter (f, w, filtering_mode, boundary_options, size_options)

Where f is the input image, w is the filter mask, g is the filtered result

Table 4.1 Filtering Mode

Options	Description
‘corr’	imfilter performs multidimensional filtering using correlation, which is the same way that filter2 performs filtering. When no correlation or convolution option is specified, imfilter uses correlation.
‘conv’	imfilter performs multidimensional filtering using convolution.

Table 4.2: Size Option:

Options	Description
‘full’	The output array is the full filtered result, and so is larger than the input array.
‘same’	The output array is the same size as the input array. This is the default behavior when no output size options are specified.

Table 4.3: Boundary Option:

Options	Description
X	Input array values outside the bounds of the array are implicitly assumed to have the value X.
'symmetric'	Input array values outside the bounds of the array are computed by mirror-reflecting the array across the array border
'replicate'	Input array values outside the bounds of the array are assumed to equal the nearest array border value.
'circular'	Input array values outside the bounds of the array are computed by implicitly assuming the input array is periodic

The example of the imfilter:

(a) (b)

Figure 4.5: (a) Image before filteration (b) Image after filteration

2. **fspecial**: The number of predefined 2-D filter linear spatial filters, obtained by using function fspecial ,which generates filter mask, h , using the syntax:

h = fspecial (type, parameters)

It accepts a filter type plus additional modifying parameters particular to the type of filter chosen. It smooth and enhance the image. The fspecial function produces several kinds of predefined filters, in the form of correlation kernels. After creating a filter with fspecial, that can apply it directly to your image data using imfilter.

The example of illustrates applying an unsharp masking filter to a grayscale image. The unsharp masking filter has the effect of making edges and fine detail in the image more crisp

Figure 4.6: (a) Original Image (b) Filtered Image using imfilter and fspecial

Table 4.4: Types of the filters:

Type	Description and Syntax
‘average’	h = fspecial('average',hsize) returns an averaging filter h of size hsize.
‘disk’	h = fspecial('disk',radius) returns a circular averaging filter (pillbox) within the square matrix of side 2*radius+1.
‘gaussian’	h = fspecial('gaussian',hsize,sigma) returns a rotationally symmetric Gaussian lowpass filter of size hsize with standard deviation sigma.
‘laplacian;	h = fspecial('laplacian',alpha) returns a 3-by-3 filter approximating the shape of the two-dimensional Laplacian operator.
‘log’	h = fspecial('log',hsize,sigma) returns a rotationally symmetric Laplacian of Gaussian filter of size hsize with standard deviation sigma
‘motion’	h = fspecial('motion',len,theta) returns a filter to approximate, once convolved with an image, the linear motion of a camera by len pixels, with an angle of theta degrees in a counterclockwise direction
‘prewitt’	h = fspecial('prewitt') returns the 3-by-3 filter h (shown below) that emphasizes horizontal edges by approximating a vertical gradient
‘sobel’	h = fspecial('sobel') returns a 3-by-3 filter h (shown below) that emphasizes horizontal edges using the smoothing effect by approximating a vertical gradient.
‘unsharp’	h = fspecial('unsharp',alpha) returns a 3-by-3 unsharp contrast enhancement filter. fspecial creates the unsharp filter from the negative of the Laplacian filter with parameter alpha negative of the Laplacian filter with parameter alpha.

(a) (b)

(c) (d)

Figure 4.7: (a) Grayscale Image (b) Image filtered by motion filter (c) image filtered by disk filter (d) Image filtered by unsharp filter.

4.3.1.2 Non -Linear Spatial Filtering:

This filtering is based on neighborhood operation and the mechanism of defining m*n neighborhood by sliding the center. This filter is based the nonlinear operations involving the pixels of a neighborhood and response constitute the response of the operation at the center pixel of the neighborhood.

The toolbox provides function for performing general non-linear filtering: n1filter, co1filt and ordfilt2.

nlfilter:

This performs directly in 2-dimensional and general sliding-neighborhood operations.

The syntax nlfilt:

B = nlfilt (A, [m n], fun)

It applies the function fun to each m-by-n sliding block of A. fun is a function that accepts an m-by-n matrix as input and returns a scalar result. c = fun(x)fun must be a function handle .c is the output value for the center pixel in the m-by-n block x. nlfilter calls fun for each pixel in A. nlfilter zero-pads the m-by-n block at the edges, if necessary.

colfilt:

This organizes the data in the column. It processes distinct or sliding blocks as columns. requires more memory and executes faster than n1filter.The syntax of the function co1filt:

B = colfilt (A, [m n], block_type, fun)

It processes the image A by rearranging each m-by-n block of A into a column of a temporary matrix, and then applying the function fun to this matrix. fun must be a function handle.

ordfilt2:

This nonlinear spatial filter response is based on ordering the pixels contained in an image neighborhood and then replacing the values of the centre pixel in the neighborhood and then replacing the value of the centre pixel in the neighborhood with the value determined by the ranking result. The syntax is:

B = ordfilt2 (A, order, domain)

It replaces each element in A by the orderth element in the sorted set of neighbors specified by the nonzero elements in domain.

For example,

B = ordfilt2 (A, 5, ones (3, 3)) implements a 3-by-3 median filter;

B = ordfilt2 (A, 1, ones (3, 3)) implements a 3-by-3 minimum filter

B = ordfilt2 (A, 9, ones (3, 3)) implements a 3-by-3 maximum filter.

B = ordfilt2 (A, 1, [0 1 0; 1 0 1; 0 1 0]) replaces each element in A by the minimum of its north, east, south, and west neighbors.

Chapter 5
Methodology

5.1 Matlab software

(MATrix LABoratory) is a programming language for technical computing from TheMath Works, Natick, MA. Used for a wide variety of scientific and engineering calculations, especially for automatic control and signal, image processing, it also have extensive graphical capabilities.

MATLAB is a high-level language and interactive environment that enables us to perform computationally intensive tasks faster than with traditional programming languages such as C, C++, and FORTRAN.

5.2 Image processing toolbox

Image Processing Toolbox is a collection of functions that extend the capability of the MATLAB numeric computing environment. The toolbox supports a wide range of image processing operations. In this work, we have used image processing toolbox of MATLAB version 7.2.

5.3 Algorithm

This algorithm is given by Chunming Li for his MATLAB code for level-set with out reinitialization. This thesis work is to modify the existing code to get better results. The description and modification that has done is described in this chapter.

Step 1-Firstly the image was read with the help of imread command. This is an inbuilt command in matlab image processing toolbox.

Syntax of the imread function:

A = imread (filename, fmt);

This reads a grayscale or color image from the file specified by the string filename, where the string fmt specifies the format of the file. If the file is not in the current directory or in a directory in the MATLAB path, specify the full pathname of the location on the system. Imread returns the image data in the array A.

Step 2 -Now the matrix values are converted into more uniform and simplify form so that further calculation can become easy with help of mathematical formula.

$$f = I x. ^2+Iy. ^2$$

Step 3_–Now the image is filtered with the help of Gaussian filter. This filter is used to remove the noise from the image so as to make image more sharp and smooth. The Gaussian filters smoothness or blurs an image by performing a convolution operation with a Gaussian filter kernel.

Syntax of the Gaussian filter:

h = fspecial (‘gaussian’, hsize, sigma)

It returns a rotationally symmetric Gaussian low pass filter of size hsize with standard deviation sigma (positive). hsize can be a vector specifying the number of rows and columns in h, or it can be a scalar, in which case h is a square matrix. The default value for hsize is [3 3], the default value for sigma is 0.5.

Step 4-In this step the gradient of the image matrix is find out. Now this gradient image is used to calculate the edges of the image.

$$[F_x, F_y]=\text{gradient } (F)$$

Gradient can be thought of as a collection of vectors pointing in the direction of increasing values of gray level. In MATLAB, numerical gradients (differences) can be computed for functions with any number of variables.

F_x = gradient (F) where F is a vector returns the one-dimensional numerical gradient of F. F_x corresponds to the differences in x (horizontal) direction.

[F_x, F_y] = gradient (F) where F is a matrix returns the x and y components of the two-dimensional numerical gradient. F_x corresponds to the differences in (horizontal) direction. F_y corresponds to the differences in the (vertical) direction. The spacing between points in each direction is assumed to be one.

Step 5-In this step all Parameters are defined which change the topology of the level-set means speed, stability etc. The parameters are alpha, time step, MU, lambda, epsilon.

Step 6-In this step, the intensity of the image is to be set with the help of the function colormap and imagesc function.

Syntax of the colormap function:

colormap (map)

A colormap is an m-by-3 matrix of real numbers between 0.0 and 1.0. Each row is an RGB vector that defines one color. If any values in map are outside the interval [0 1], MATLAB returns the error Colormap must have values in [0, 1].

Syntax of the image function:

Imagesc(C) and imagesc(x,y,C)

The imagesc function scales image data to the full range of the current colormap and displays the image. Imagesc(C) displays C as an image. Each element of C corresponds to a rectangular area in the image.

Step7-Initialization of level-set means starting shape of level-set which is depending upon the region. Mainly it has to start from the centre of part in medical image because in medical images their many other body parts of body make many edges so if it start from outside the image or tumor then it stop on other edges not on the edge of required part. So in this it start from center by making a polygon by mouse click inside the required part using this command. It creates a polygon and this value has to give to level-set function.

Step 8- In this step we gave all parameters and the initial level-set to the evolution function. This evolution function updates the level set function according to the level set evolution. The simple idea of the curve evolution is to reduce the set of vertices of the polygon to a subset of vertices containing important information about the original level-set.

Step 9- The step 8 repeat until we will not get final level-set. The repetition is depending on the number of iteration given.

Step 10- In last step, final level-set will display after all iterations. The updated value from evolution function is given to the function level-set and at end of the iterations it gives us final level-set.

5.4 Modified algorithm

There are many changes made in this algorithm and this algorithm gives better results than previous .Different filters are used to modify the image and also many parameters are to be calculated to find the most suitable filter for the segmentation of the biomedical images.

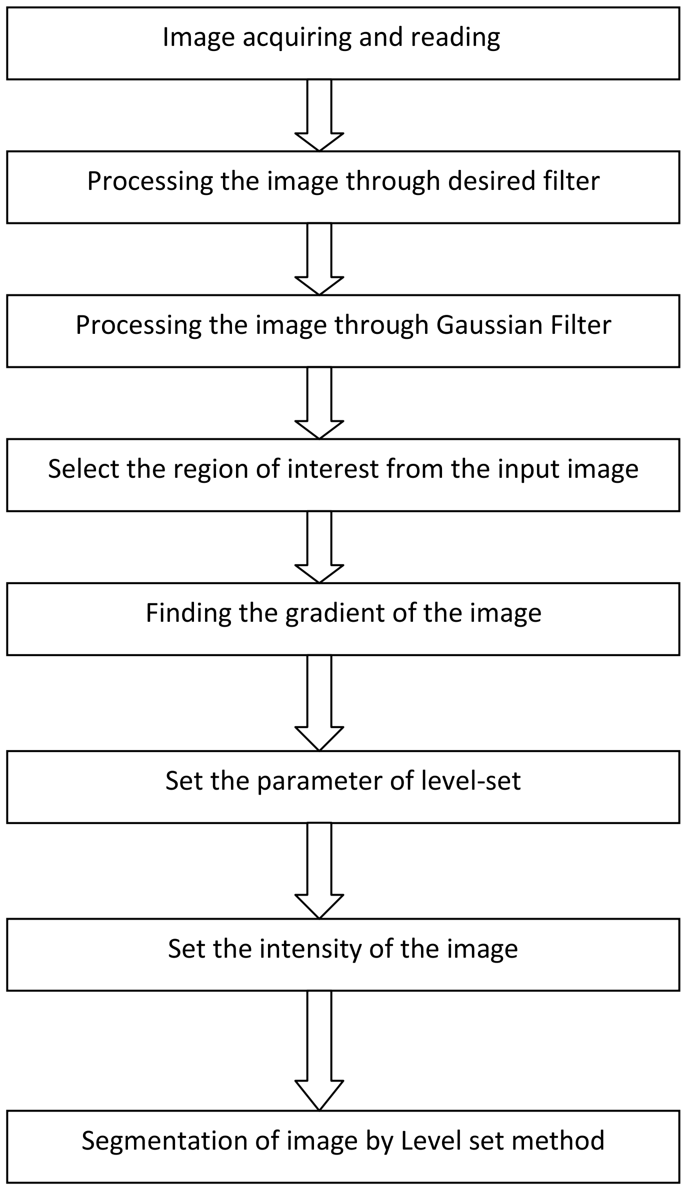

Figure 5.1: Block diagram of the modified algorithm

These are the following changes made in the algorithm:

1. The different filters were used to filter the image. The filters were used before the Gaussian filter. This technique is used to modifying or enhancing an image. It helps to emphasize certain features or remove other features of the image .It smoothness, sharpening and enhancement the edge of the image.

Basically two types of filtering techniques were used:

- Linear filtering
- Non –linear filtering

(i) Linear filtering: Linear filtering is filtering in which the value of an output pixel is a linear combination of the values of the pixels in the input pixel's neighborhood. Linear filtering is done through the matlab function of fspecial and imfilter.

(a) fspecial: It creates 2-D special filters

Syntax of fspecial:

h= fspecial (type)

h = fspecial (type, parameters)

h = fspecial (type) creates a two-dimensional filter h of the specified type. ‘fspecial’ returns h as a correlation kernel, which is the appropriate form to use with imfilter. ‘type’ is a string having the of one of these filters.

(b) imfilter: It performs multidimensional image filtering.

Syntax of imfilter:

B = imfilter (A, H)

It is a multidimensional array A with the multidimensional filter H. The array A can be a nonsparse numeric array of any class and dimension. The result B has the same size and classes A. Each element of the output B is computed using double-precision floating point. If A is an integer array, then output elements that exceed the range of the integer type are truncated, and fractional values are rounded. ‘imfilter’ is more memory efficient than some other filtering operations in that it outputs an array of the same data type as the input image array.

One of the examples how linear filtering is performed.

H=fspecial ('unsharp');

B=imfilter (I, H);

(ii). **Non-linear filtering**: This filtering is more effective than Linear filtering and it is used to reduce noise and preserve edges.

ordfilt2: It 2-dimensional order-statistic filtering

Syntax:

B = ordfilt2 (A, order, domain)

It replaces each element in A by the orderth element in the sorted set of neighbors specified by the nonzero elements in domain.

2. To increase the intensity of the image the parameters controlling the intensity has been adjusted.

3. Now call the selection base program. This program chooses the appropriate values of level-set parameters form its database according to the if-else rules .The output of this control strategy are the input for the segmentation program. The parameters alfa, lamda, sigma, epsilon are the optimized parameter for the level set program.

4. The height, length and the area of the segmented part can be calculated. Segmented-area equals to the area of the closed curve when it is in anti-clockwise and equals to the negative area when it is in clockwise. Negative area means equal to area in magnitude but is negative in sign. It used to judge the direction of a closed curve. C provides the coordinates of the nodes of the curve

Area =varea(C)

Area returns the area of the curve (>0) when it is in anti-clockwise and negative area of the curve (<0) when it is in clockwise.

5. Next step is to calculate the following parameters of the filtered image and the original image.

- Signal to noise ratio (SNR)

  It compares the level of desired signal to the level of background noise. The higher the ratio, the less obtrusive the background noise
- Peak signal to noise ratio (PSNR)

  It is the ratio between possible power of a signal and the power of corrupting noise that affects the fidelity of its representation.
- Weighted peak signal to noise ratio(WPSNR)
- Entropy

CHAPTER 6

SIMULATION AND TESTING

6.1 Introduction

This chapter elaborates the simulation and testing part of our thesis. It describes the various steps taken in the development of the program and then the testing of the program with various biomedical images.

6.2 Test results for MRI image 1 with various filters

Figure 6.1: Original MRI image 1

Dimension of segmented area when no filter is used

Width: 69.7 pixels

Height: 59.1 pixels

Area of closed curve: 4.8654e+003

Table 6.1: Dimensions of segmented area of MRI image 1 with various filters

Type of Filter	Images	Width	Height	Area of segmented part	Result
Maximum filter		68.0	58.6	4.7012e+003	The area of segmentation has increased and nearly entire desired area is segmented.

Median filter	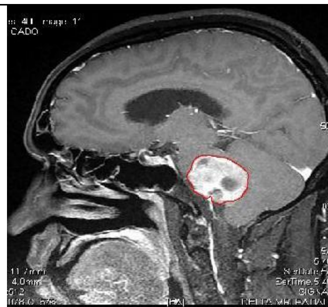	62.0	35.5	4.6230e+003	The area of segmentation has increased but fails to segment the entire desired area.
Minimum filter		64.0	51.0	4.4256e+003	This filter fails to segment the entire desired area.
Log filter		35.7	28.9	1.8230e+003	This filters segment very less area therefore the filter is not suitable for such type of segmentation
Average filter		63.3	48.3	3.6087e+003	The area of segmentation has increased but filter fails to segment the desired area.
Laplacian filter	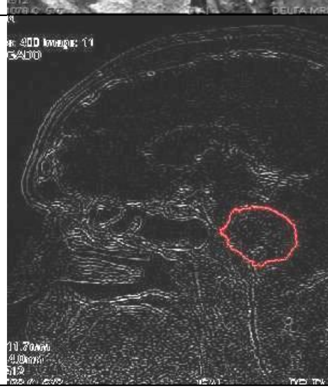	59.1	46.0	5. 021e+003	The filters crosses the boundaries of segmented area therefore it is not suitable for such type of segmentation

Prewitt filter	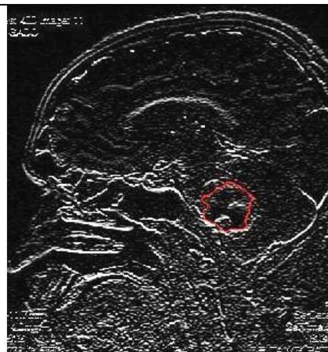	47.7	42.2	2.1181e+003	The area of segmentation has increased but filter fails to segment the desired area.
Sobel filter		37	30.1	1.7497e+003	The area of segmentation is very small therefore the filter is not suitable for such type of segmentation .
Unsharp filter		40.1	24.5	2.2532e+003	The area of segmentation is very small therefore this filter is not suitable for such type of segmentation .
Disk filter	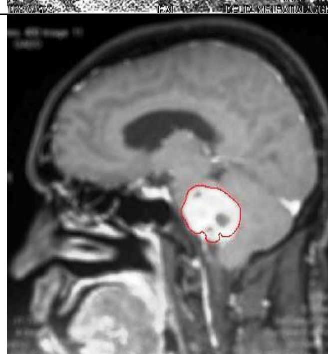	63.9	50.3	4.6385e+003	The area of segmentation has increased but filter fails to segment the desired area.
Motion filter	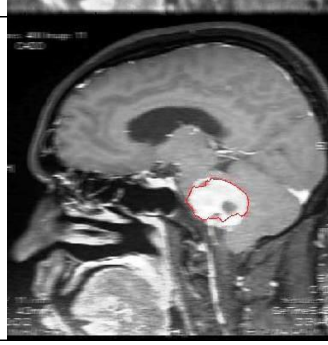	64.5	43.7	3.8522e+003	By the use of this filter the area of segmentation has decreased.

Gaussian filter	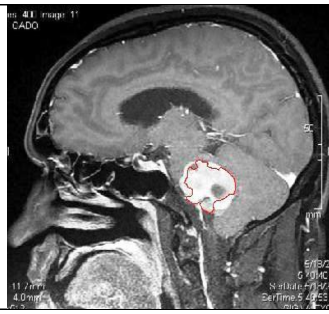 52.3	47.5	3.3639e+003	This filter fails to segment the entire desired part.

Table 6.2: Parameters of MRI image 1 of various filters:

Images	SNR	PSNR	WPSNR	ENTROPY
Maximum filter	14.0377	14.5137	8.4931	5.5297
Median filter	11.2798	11.7558	5.73252	5.5295
Minimum filter	9.9093	10.3853	4.3647	5.5300
Log filter	2.2987	2.7746	0.4152	4.0462
Average filter	13.1044	13.5803	8.0775	5.5703
Laplacian filter	2.2494	2.7254	0.2958	3.6277
Prewitt filter	2.4453	2.9213	0.5408	6.3965
Sobel filter	2.4759	2.9519	0.1275	4.1403
Unsharp filter	10.2706	10.7466	5.9742	5.4583
Disk filter	11.0849	11.5609	5.3248	4.9076
Motion filter	12.4978	12.9737	6.3302	5.5832
Gaussian filter	15.7458	16.2217	15.0941	5.5848

6.3 Test results for MRI image 2 with various filters

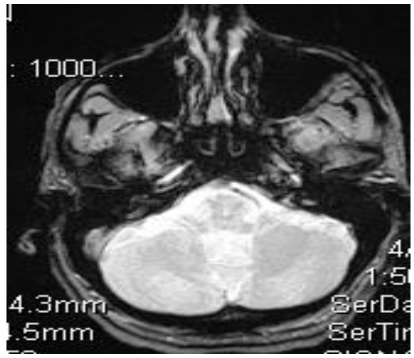

Figure 6.2: Original image of MRI 2

Dimension of segmented area when no filter is used

Width: 175.6 pixels

Height: 96.7 pixels

Area of closed curve: 5.9856e+003

Table 6.3: Dimensions of segmented area of MRI image 2 with various filters:

Type of Filter	Images	Width	Height	Area of segmented part	Result
Maximum filter		173.1	95.8	5.8144e+03	The area of segmentation has increased and nearly entire desired area is segmented.
Median filter		171.6	93.4	5.8035e+003	The area of segmentation has increased but fails to segment the entire desired area.

Minimum filter	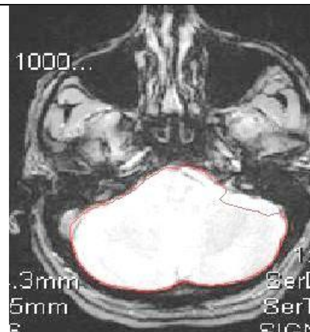	167.6	91.0	5.5413e+003	This filter fails to segment the entire desired area.
Log filter	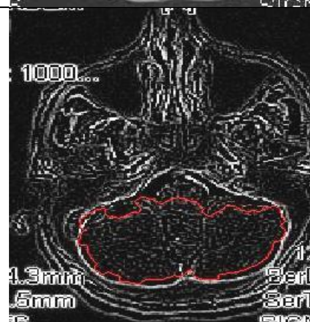	170.6	66.5	4.2858e+003	This filters segment very less area and the filter is not suitable for such type of segmentation
Average filter	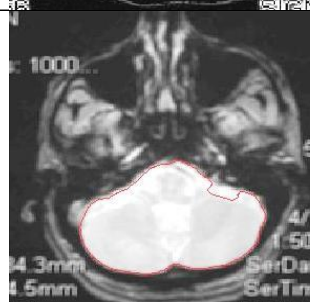	169.9	92.0	5.4652e+003	The area of segmentation has increased but filter fails to segment the desired area.
Laplacian filter	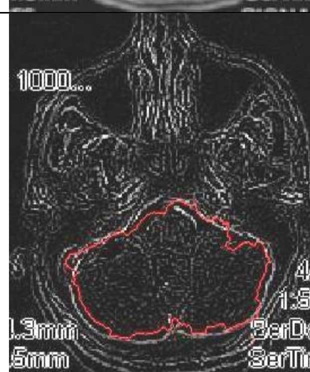	164.0	93.8	1.6088e+004	The filters crosses the boundaries of segmented area therefore it is not suitable for such type of segmentation
Prewitt filter	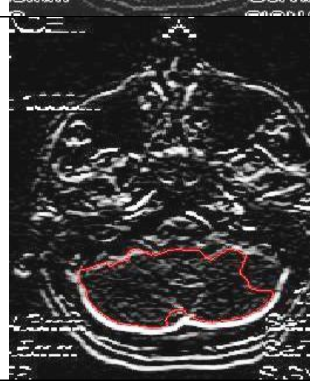	155.1	50.0	3.3551e+003	The area of segmentation has increased but filter fails to segment the desired area.

Sobel filter	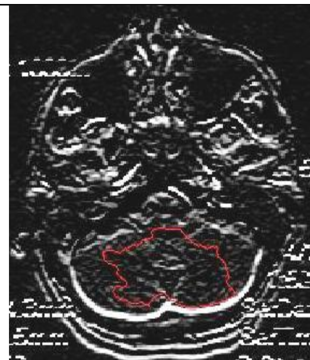	93.4	51.5	2.1302e+003	The area of segmentation is very small therefore the filter is not suitable for such type of segmentation .
Unsharp filter		162.7	68.0	3.0532e+003	The area of segmentation is very small therefore this filter is not suitable for such type of segmentation .
Disk filter		174.8	92.2	5.6542e+003	The area of segmentation has increased but filter fails to segment the desired area.
Motion filter	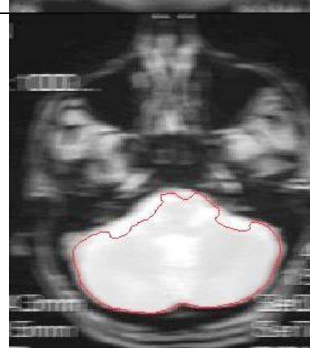	169.6	84.2	5.2221e+003	By the use of this filter the area of segmentation has decreased.
Gaussian filter	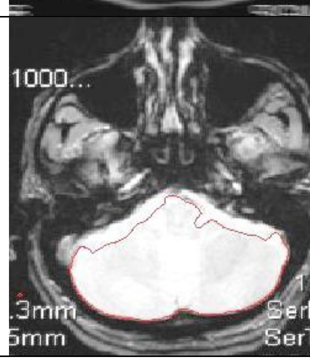	167.0	86.5	4.3499e+003	This filter fails to segment the entire desired part.

Table 6.4: Parameters of MRI image 2 of various filters:

Images	SNR	PSNR	WPSNR	ENTROPY
Maximum filter	12.9768	13.5768	9.8765	4.5947
Median filter	10.9787	11.7798	7.3251	4.5946
Minimum filter	10.1276	11.3712	7.1234	4.5929
Log filter	1.9332	3.2478	0.1546	3.9745
Average filter	10.0450	11.3596	6.9499	4.9546
Laplacian filter	1.8595	3.1741	0.4533	3.6142
Prewitt filter	2.0717	3.3864	1.3145	3.3774
Sobel filter	2.1197	3.4343	1.1848	3.5151
Unsharp filter	7.9920	9.3067	9.7238	4.4494
Disk filter	6.8121	8.1267	6.1486	5.1569
Motion filter	8.9791	10.2937	6.8307	5.0480
Gaussian filter	10.8710	12.1857	9.7889	4.8658

6.4 Test results for X- ray image 1 with various filters

Figure 6.3: Original image of X-ray

Dimension of segmented area when no filter is used

Width: 43.4 pixels

Height: 51.7 pixels

Area of closed curve: 4.009e+003

Table 6.5: Dimensions of segmented area of X-ray image 2 with various filters:

Type of Filter	Images	Width	Height	Area of segmented part	Result
Maximum filter		41.49	49.03	3.7256e+003	The area of segmentation has increased and nearly entire desired area is segmented.
Median filter		37.59	49.01	2.9039e+003	The area of segmentation has increased but fails to segment the entire desired area.

Minimum filter		30.91	39.16	2.2367e+003	This filter fails to segment the entire desired area.
Log filter		30.15	32.06	1.7580e+003	This filters segment very less area therefore the filter is not suitable for such type of segmentation
Average filter		27.31	38.47	2.2625e+003	The area of segmentation has increased but filter fails to segment the desired area.
Laplacian filter	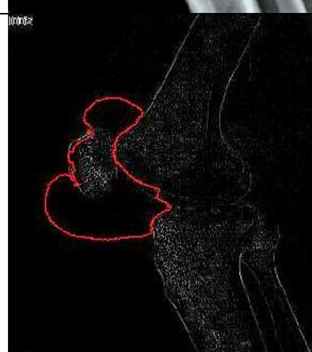	85.02	109.09	1.3723e+003	The filters crosses the boundaries of segmented area therefore it is not suitable for such type of segmentation
Prewitt filter		25.48	21.36	1.3520e+003	The area of segmentation has increased but filter fails to segment the desired area.

Sobel filter		22.39	27.35	1.3534e+003	The area of segmentation is very small therefore the filter is not suitable for such type of segmentation.
Unsharp filter		27.52	31.10	2.0053e+003	The area of segmentation is very small therefore this filter is not suitable for such type of segmentation.
Disk filter		39.09	44.50	3.3242e+003	The area of segmentation has increased but filter fails to segment the desired area.
Motion filter		28.28	25.50	1.5961e+003	By the use of this filter the area of segmentation has decreased.
Gaussian filter		29.73	38.28	2.1387e+003	This filter fails to segment the entire desired part.

Table 6.6: Parameters of X-ray of various filters:

Images	SNR	PSNR	WPSNR	ENTROPY
Maximum filter	14.0377	14.5137	8.4931	4.5435
Median filter	11.2798	11.7558	5.7352	4.4324
Minimum filter	9.9093	10.3853	4.3647	4.4320
Log filter	1.8548	4.3814	1.0428	3.2215
Average filter	10.4712	12.9998	10.2184	4.5206
Laplacian filter	1.8044	4.3330	1.1826	2.9717
Prewitt filter	2.4346	4.9632	1.5869	3.0008
Sobel filter	2.4507	4.9793	1.5670	3.1439
Unsharp filter	13.1962	15.7248	9.4553	4.4683
Disk filter	8.5383	11.0669	8.0045	4.6513
Motion filter	9.6280	12.1566	9.1290	4.5584
Gaussian filter	11.6451	14.1737	17.8616	4.5320

6.5 Test results for CT images with various filters

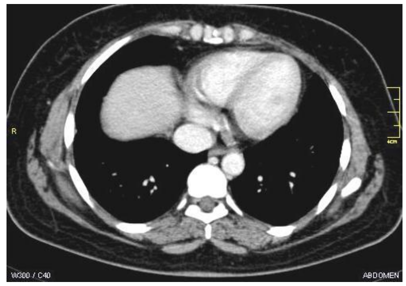

Figure 6.4: Original image of CT image

Dimension of segmented area when no filter is used

Width: 43.6 pixels

Height: 26.9 pixels

Area of closed curve: 1.8067e+003

Table 6.7: Dimensions of segmented area of CT image with various filters:

Type of Filter	Images	Width	Height	Area of segmented part	Result
Maximum filter	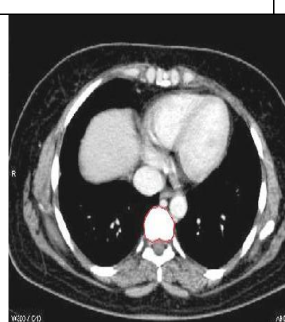	42.3	25.7	1.7969e+003	The area of segmentation has increased and nearly entire desired area is segmented.
Median filter	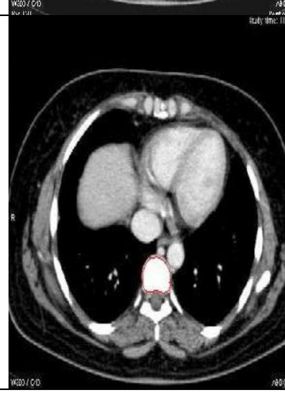	38.9	23.3	1.6161e+003	The area of segmentation has increased but fails to segment the entire desired area.

Minimum filter	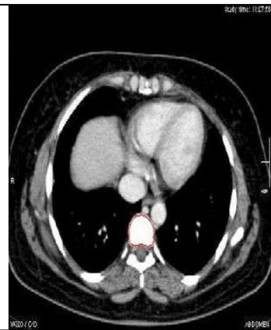	40.1	21.8	1.5924e+003	This filter fails to segment the entire desired area.
Log filter	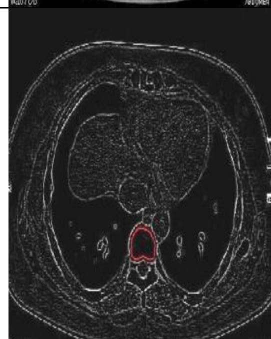	35.2	19.8	1.2468e+003	This filters segment very less area therefore the filter is not suitable for such type of segmentation
Average filter	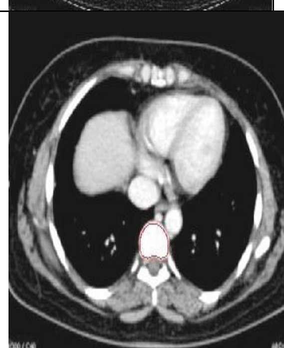	38.6	22.7	1.4812e+003	The area of segmentation has increased but filter fails to segment the desired area.
Laplacian filter	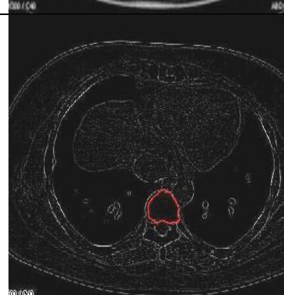	38.9	28.2	1.9782e+003	The filters crosses the boundaries of segmented area therefore it is not suitable for such type of segmentation
Prewitt filter		38.0	24.7	1.4008e+003	The area of segmentation has increased but filter fails to segment the desired area.

Sobel filter			35.2	19.1	1.1365e+003	The area of segmentation is very small therefore the filter is not suitable for such type of segmentation.
Unsharp filter		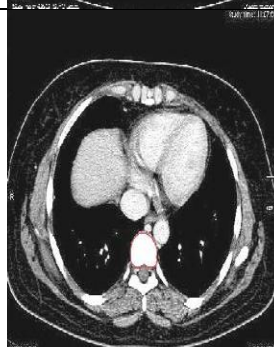	40.7	23.6	1.6483e+003	The area of segmentation is very small therefore this filter is not suitable for such type of segmentation.
Disk filter		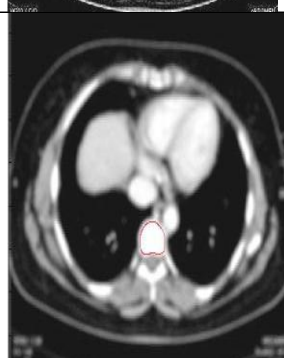	36.9	21.7	1.3748e+003	The area of segmentation has increased but filter fails to segment the desired area.
Motion filter		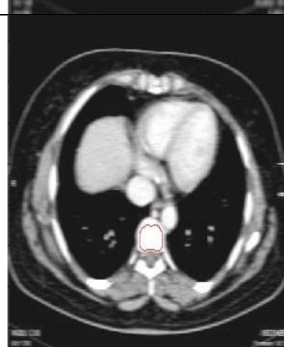	34.5	19.1	3.8522e+003	By the use of this filter the area of segmentation has decreased.
Gaussian filter		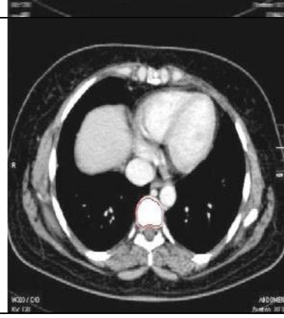	37.3	23.3	1.4265e+003	This filter fails to segment the entire desired part.

Table 6.8: Parameters of CT image of various filters:

Images	SNR	PSNR	WPSNR	ENTROPY
Maximum filter	14.0377	14.5137	8.4931	6.1030
Median filter	11.2798	11.7558	5.7352	5.9055
Minimum filter	9.9093	10.3853	4.3647	5.5253
Log filter	1.8548	4.3814	1.0428	5.4555
Average filter	10.4712	12.9998	10.2184	6.0955
Laplacian filter	1.8044	4.3330	1.1826	4.7950
Prewitt filter	2.4346	4.9632	1.5869	5.2886
Sobel filter	2.4507	4.9793	1.5670	5.4321
Unsharp filter	13.1962	15.7248	9.4553	6.1278
Disk filter	8.5383	11.0669	8.0045	6.0283
Motion filter	9.6280	12.1566	9.1290	6.0071
Gaussian filter	11.6451	14.1737	17.8616	6.0548

CHAPTER 7

CONCLUSION AND FUTURE SCOPE

Conclusions

The process of segmentation of biomedical images requires a very high degree of accuracy while we are dealing with something as serious as a brain tumor, any little mistake can put patient's life in risk.

To overcome this problem, many efforts have been made by the researchers across the globe for last many years. A similar effort has been made in this thesis to analyze the various filtering techniques and to find out the best among the twelve filters. The setup has been tested for different biomedical images such as CT scan MRI and X- rays. In the process of final evaluation we found that the results for CT scan and MRI images were good as compared to X ray images. Out of the twelve filters used, maximum filter did the best job as far as segmentation of MRI and CT images are concerned. It may be concluded that the project has been by and far successful.

Future Scope

Though we have achieved better results in case of CT scan and MRI images but still the system failed in case of Ultrasound images due to the presence of speckle noise in ultrasound. Therefore, to make the system work for Ultrasound images special filter needs to be developed and further optimization is required.

REFERENCES

[1] Lucas Lorenzo , MacLeod, S. Robert Adluru and Ganesh “Level sets and shape models for segmentation of cardiac perfusion MRI” Computerized Medical Imaging and Graphics, Volume 6144, pp. 1320-1331 ,1998.

[2] Sven Loncaric, M.Subasic and E.Sorantin. “3-D deformable model for aortic aneurysm segmentation from CT images” Engineering in Medicine and Biology Society, Vol: 1, pp: 398-401, 2000.

[3] C.F Westin, J. Richolt, V. Moharir and R. Kikinis “Affine Adaptive Filtering of CT Data” Medical Image Analysis, Vol: 4, No. 2, pp: 161-172 , June 2000.

[4] C. Baillard, P. Hellier and C. Barillot, “Segmentation of 3D brain structures using level sets and dense registration” Mathematical Methods in Biomedical Image Analysis, pp: 94-101, 2000.

[5] M. Droskey, B. Meyerz, M. Rumpfy and K. Schallerz “An adaptive level set method for medical image segmentation” IEEE Transactions on In Medical Imaging,Vol. 2, No. 2. pp. 37-42, 2001

[6] Hongchuan Yu “An Adaptive Level Set Method for Medical Image Segmentation” Inter national workshop on Information Processing in Medical Imaging, Vol: 2082, pp: 416-422, 2001.

[7] Nathan Moon “Automatic Brain and Tumor Segmentation” Medical Image Computing and Computer-Assisted Intervention”, Vol: 2488, pp: 372-379,2002.

[8] Nikos Paragios “A Variational Approach for the Segmentation of the Left Ventricle in Cardiac Image Analysis” International Journal of Computer Vision, Vol: 50, pp: 345 – 362, December 2002.

[9] L. Zhukov, K. Museth, D. Breen, R. Whitaker and A. Barr, ``Level Set Modeling and Segmentation of DT-MRI Brain Data," Journal of Electronic Imaging, Vol. 12, No. 1, pp. 125-133, January 2003.

[10] A Tsai, A Yezzi, W Wells, C Tempany, D Tucker, A Fan, WE Grimson, A Willsky “A shape-based approach to the segmentation of medical imagery using level sets “IEEE Transactions on In Medical Imaging, Vol. 22, No. 2. pp. 137-154 , 2003.

[11] Hossam Hassan and Farag, “MRA data segmentation using level sets” International Conference on Image Processing, Vol: 2, pp: 173-176 sept.2003.

[12] D. Metaxas, T. Chen, X. Huang and L. Axel “Cardiac Segmentation from MRI-Tagged and CT Images”, IEEE Computer Conference on IEEE Computer Conference on Computer Vision and Pattern Recognition, Vol. 4, pp 78-82, 2004.

[13] Qigong Zhang “Segmenting Cardiopulmonary Images Using Manifold Learning with Level Sets” Computer Vision for Biomedical Image Applications, Vol: 3765, pp: 479-488, 2005.

[14] Y Chenoune, E Delechelle, E Petit, T Goissen, J Garot and A Rahmouni “Segmentation of cardiac cine-MR images and myocardial deformation assessment using level set methods:”Computerized Medical Imaging and Graphics, Vol. 29, No. 8, pp. 607-616 , 2005.

[15] Chunming Li , Chenyang Xu and Changfeng Gui “Level set evolution without re-initialization: a new variational formulation” IEEE Computer Conference on Computer Vision and Pattern Recognition, Vol :1 , pp: 430-436, 2005.

[16] Seongjai Kim and Hyeona Lim “A hybrid level set segmentation for medical imagery”IEEE Symposium Conference on Nuclear Science Record, Volume: 3, pp: 5-9, Oct 2005.

[17] R. Manniesing , B.K. Velthuis , M.S. van Leeuwen, I.C. van der Schaaf, P.J. van Laa and W.J. Niessen “Level set based cerebral vasculature segmentation and diameter quantification in CT angiography” IEEE Computer Conference on Recognition, Vol :3,pp: 89-95, 2005.

[18] Seong-Jae Lim, Yong-Yeon Jeong and Yo-Sung Ho “Automatic liver segmentation for volume measurement in CT Images” IEEE Computer Conference on Computer Vision and Pattern Recognition , pp: 860-875, 2006.

[19] Shaojun Liu and Jia Li “Automatic Medical Image Segmentation Using Gradient And Intensity Combined Level Method” IEEE Annual International Conference on Medical Imaging, pp: 78-82, 2006.

[20] Qigong Zhang and R. Souvenir. “On Manifold Structure of Cardiac MRI Data: Application to Segmentation” IEEE Computer Society Conference on Computer Vision and Pattern Recognition, Vol: 1, pp: 1092- 1098, June 2006.

[21] Elsa Angelin, Song Ting and A. Laine. “Homogeneity measures for multiphase level set segmentation of brain MRI” IEEE International Symposium on Biomedical Imaging ,pp: 746-749, April 2006.

[22] Xujia Qin , Jionghui Jiang , Weihong Wang and Fan Zhang “Canny Operator Based Level Set Segmentation Algorithm for Medical Images”. International Conference on Bioinformatics and Biomedical Engineering, pp: 892-895, 2007.

[23] D.R. Bathula. , X. Papademetris and J.S. Duncan “Level set based clustering for analysis of functional MRI data” IEEE International Symposium on Biomedical Imaging: pp 416-419, April 2007.

[24] Jeongjin Lee, Namkug Kim, Ho Lee, Joon Beom Seo, Hyung Jin Won, Yong Moon Shin, Yeong-Gil Shin and Soo-Hong Kim “ Efficient liver segmentation using a

level-set method with optimal detection of the initial liver boundary from level-set speed images". Computer Methods and Programs in Biomedicine, Vol: 1, pp: 26-38, 2007.

[25] Gunnare Lathen, J. Jonasson and M.Borga. "Phase based level set segmentation of blood vessels" International Conference on Pattern Recognition, pp: 1-4, 2008,

[26] P.C. Pedersen, J.D. Quartararo, and T.L. Szabo, "Segmentation of Speckle-Reduced 3D Medical Ultrasound Images," IEEE Ultrasonics Symposium Proceedings, pp: 56-63, 2008,

[27] Xie, Qiangjun Chen, Xufeng Ma, Li Zhou, Zekui "Segmentation for CT Image Based on Improved Level-Set Approach" Conference on Image and Signal Processing, Vol: 3, pp: 725-728, May 2008

[28] Jakub Kratky and Jan Kybic "Three-dimensional segmentation of bones from CT and MRI using fast level sets" Information Processing in Medical Imaging, Vol: 6914, pp: 57-47, 2008

[29] S. Randrianarisolo, E. Delechelle, E. Petit, A.Rahmouni and J.Garot "Assessment of myocardial deformations from untagged cardiac cine MRI" International Conference of the IEEE on Engineering in Medicine and Biology Society, pp: 3401-3404, 2008.

[30] Laurent Massoptier and Sergio Casciaro "A new fully automatic and robust algorithm for fast segmentation of liver tissue", 2008.

[31] Gang Chen, Lixu Gu , Lijun Qian and Jianrong Xu "An Improved Level Set for Liver Segmentation and Perfusion Analysis in MRIs"IEEE Transactions on Information Technology in Biomedicine, Vol: 13, pp:94-103, Jan. 2009,